ResearchGate

See discussions, stats, and author profiles for this publication at: https://www.researchgate.net/publication/387412442

Optimisation of desalination-based water system with integrated renewable energy and storage within the water-energy nexus

Article *in* Desalination · December 2024

DOI: 10.1016/j.desal.2024.118474

CITATIONS
0

READS
34

2 authors:



Goran Stunjek
University of Zagreb
10 PUBLICATIONS **94** CITATIONS

SEE PROFILE



Goran Krajacic
University of Zagreb
193 PUBLICATIONS **5,274** CITATIONS

SEE PROFILE

All content following this page was uploaded by Goran Stunjek on 02 January 2025.

The user has requested enhancement of the downloaded file.

Optimisation of Desalination-Based Water System with Integrated Renewable Energy and Storage within the Water-Energy Nexus

Goran Stunjek*, University of Zagreb, Faculty of Mechanical Engineering and Naval Architecture, Croatia
goran.stunjek@fsb.hr

Goran Krajačić, University of Zagreb, Faculty of Mechanical Engineering and Naval Architecture, Croatia
goran.krajacic@fsb.hr

https://doi.org/10.1016/j.desal.2024.118474

Abstract

This study presents a comprehensive optimization framework for integrated water and energy systems. It offers a novel implementation to determining the optimal dispatch of water and energy streams and sizing Battery Energy Storage (BES)[1] and Renewable Energy Systems (RES)[2]. The proposed Mixed-Integer Linear Programming model integrates RES and BES with water systems through Reverse Osmosis desalination units and water storage supported by Power-to-Water technology. Unlike traditional models, the framework considers both BES capacity and power rating as variables while incorporating RES capacity optimization, water system modelling, and water storage integration. The integrated water-energy system model is particularly suited to addressing the unique challenges of smaller-scale island systems, often overlooked in larger-scale analyses. The methodology is applied to Unije Island, Croatia, characterized by significant seasonal demand fluctuations due to tourism. The results demonstrate the effectiveness of power-to-water and BES technology in increasing system flexibility and economic performance and provide a comprehensive analysis of the impact of varying RES and BES investment costs on optimal system configuration, and financial and economic outcomes. Lower RES investment costs lead to higher RES capacities, but the rate of change is significantly influenced by BES investment costs, highlighting the importance of an optimal RES-BES pair for maximizing financial and economic performance. Furthermore, the results emphasize that the highest financial and economic benefits are achieved not by maximizing both RES and storage capacities, but by finding an optimal balance between them, demonstrating the critical role of BES and water storage utilization in enhancing system efficiency. Change in specific parameters showed that grid electricity and PV potential effect final system profitability more than change in water demand defining two parameters as critical. Proposed study offers valuable insights into the optimization of water-energy systems on islands and other isolated regions, emphasizing the importance of integrated planning for sustainable development, and offering strategic insights for future infrastructure development.

Keywords: water-energy nexus, desalination, renewable energy sources, battery energy storage, power-to-water, flexibility

1. Introduction

All nations have agreed to reduce emissions in accordance with the goals of the Paris Agreement in order to keep global warming below 2 °C and, if at all possible, to keep it to 1.5 °C. A significant revamp of the EU's energy policy framework was launched to transition away from the heavy reliance on fossil fuels, building on the pledges made in the Paris Agreement. The eight pieces of legislation that make up the "Clean Energy for all Europeans" package [1] collectively represent the last steps in putting into practice the five pillars of the energy union strategy: security, solidarity, and trust; a fully integrated energy market; increased energy efficiency; climate action; and decarbonization; as well as research, innovation, and competitiveness [2].

[1] BES – Battery Energy Storage
[2] RES – Renewable Energy storage

The EU has more than 2,200 inhabited islands, and most of them have access to some form of renewable energy sources (RES), mostly wind and solar energy. However, many islands are still dependent on expensive imported energy sources, fossil fuels, and land-based energy supplies [3]. The EU has recognized the renewed need for island development with the legislative frameworks such as the "Smart Islands Declaration" [4] as the most important document for island development, and the "Clean Energy for European Islands" initiative [5]. The redevelopment of the island is a challenge due to the different geographical locations of the islands, different interests and requirements of the local population, and this challenge is recognized as an opportunity to learn, develop and implement new technologies. The Clean Energy for European Islands aims to reduce energy costs and increase energy production from RES, promote energy storage using the latest technologies to ensure better energy independence of the island, improve air quality, reduce greenhouse gas emissions and encourage economic transition in the context of job creation and business opportunities.

1.1. Renewable energy systems and storage integration

The integration of RES at the island level has been extensively studied. One of the pioneering approaches, the RenewIsland method, employs a four-step analysis to integrate energy and resource flows, demonstrated in case studies of Corvo, Porto Santo, and Mljet [6]. Further research explored interconnecting island groups to enhance RES utilization, incorporating electric vehicles as storage via vehicle-to-grid systems. This analysis used EnergyPLAN for scenario simulations and MultiNode for interconnection studies [7]. Similarly, [8] examined energy and transport sector integration on a carbon-neutral island reliant on intermittent RES, using EnergyPLAN to model power, cooling, heating, and transport systems. Another study developed an integrated energy system model with PLEXOS for a typical Caribbean island, incorporating power, transport, cooling, and water desalination sectors to achieve high RES penetration [9].

In [10] a review of energy storage and demand side management (DSM) highlighted the role of grid flexibility through storage, supply solutions, and sector integration. Flexible water systems and reverse osmosis (RO) based desalination were noted as key for remote islands, enabling electricity storage as water and reducing seasonal peak loads. In study [11], six hybrid RES-based RO configurations, combining wind, photo-voltaic (PV), battery energy storage (BES), and hydrogen storage, were proposed. An optimization problem is introduced where number of BES and hydrogen storage units represent two integer variables while wind turbine swept area and PV plant area represent two continuous variables. The study [12] evaluates the integration of PV system to sustainably power RO desalination units on Nisyros Island, addressing water scarcity while reducing environmental impacts. It highlights a scalable solution for other Mediterranean islands with abundant renewable energy resources. Authors in [13] present optimization model for minimizing energy consumption in micro water-energy systems, integrating RES and storage solutions. It highlights the potential of synchronized water and energy management to enhance efficiency and sustainability in interconnected systems. Although Mixed-Integer Linear Programming (MILP) optimisation approach with inclusion of BES and water storage was used, the proposed study lacks the optimisation of RES capacities which are used as parameters. A MILP model for optimizing the energy–water–carbon nexus in remote AC/DC microgrids, focusing on integrating RES and BES was developed in [14]. Similarly, even though study includes both water and energy system, as well as the energy and water storage, it is limited as RES capacities are parameters and only 24h analysis is suggested.

A study [15] examines the impact of energy and water storage on the co-optimization of water and power networks, introducing ramping constraints and storage facilities to enhance efficiency. Study suggests that only co-optimisation was performed, while power and storage capacities are represented as parameters. A hybrid RES microgrid in study [16] integrates PV, wind turbines, storage options, and RO desalination to meet electricity and potable water demands. Utilizing Particle Swarm Optimisation (PSO) approach, the system demonstrates technical feasibility and financial viability for small islands. However, RES capacities were used as parameters. Study [17] introduced a novel DSM model for the Cres-Lošinj archipelago, considering grid limitations. Results showed DSM activation at incentives below 23% of day-ahead market prices, suggesting benefits for all stakeholders from distribution-level DSM implementation. The authors in [18] applied PSO to optimize a PV-based pumping system with

hydro storage for a rural village in Nigeria. Only BES capacity was used as variable and simpler 24h only hour optimisation was proposed. A optimal dispatch integrating RES, desalination, and brine storage was done in [19]. The method was tested on a hypothetical case of Jordan for different levels of installed wind and PV capacities, as well as different sizes of the brine storage. However, no capacity optimisation was performed.

An optimization approach for the placement, sizing, and daily operation of BES to address challenges in distribution networks with high PV penetration was proposed in [20]. A proposed optimisation lacks in not having the hourly BES power variable and assumes only 1 daily charge and discharge rate. Daily curve is further multiplied by 365 to represent yearly distribution which limits the study approach. Furthermore, RES capacities are represented as parameters. Focus on optimal BES planning in distribution grids with RES to minimize costs and meet technical constraints was proposed in [21]. The study uses a hybrid tabu search/PSO algorithm to determine the ideal location, capacity, and power rating of BES. Although it uses both BES capacity and power as variable, it lacks as RES capacities are used as parameters and only 24h is proposed. Furthermore, it limits BES operation to only one daily charge/discharge operation and allows BES discharge only if BES is on max capacity.

Authors in [22] propose a MILP method for optimizing the BES capacity in a multi-energy complementary system with wind, PV, and concentrating solar power. It uses both BES capacity and power as variables, and limits BES charge and discharge with binary variables. Although similar to our proposed modelling approach, it lacks in having RES as parameters. A study [23] presents an algorithm for the simultaneous optimal sizing, placement, and operational strategy of decentralized BES systems in medium voltage distribution grids. Approach uses both BES capacity and power as variable but lacks in only having 24h horizon which is further simulated to whole year period. Objective function lacks the BES power variable, while RES capacities are parameters. A method to co-optimize BES and thermal energy storage capacities in a multi-RES-energy complementary system was proposed in [24]. Using a MILP model, it aims to maximize the system's annual profit while considering energy curtailment and operational constraints. Although suggesting that RES capacities are part of the objective function, it seems that RES capacities are used as parameters. Furthermore, only BES capacity is in objective function without BES power variable. It uses binary variables for BES charge/discharge operation. The authors in [25] present an integer-programming model for optimizing the mix of RES, conventional generation, and BES. The model minimizes capital, operational, and utility costs while meeting system constraints and demand. Although it uses both BES capacity and power as variable in objective function, RES capacity is used as parameter and no investment cost is in objective function. Additionally, no water storage is accessed. Still, study offers high level BES modelling as a main problem evaluation.

A MILP model for planning a local community's water and energy resources, focusing on the energy-water-carbon nexus was proposed in [26]. The model optimizes the sizing of components such as RES and desalination plants while minimizing costs and carbon emissions. Both BES capacity and power are variables and modelled in objective function as investment cost, but BES is limited for daily usage avoid the possibility to take seasonality into consideration. Still, binary variables were used for BES charging and discharge. Furthermore, proposed analysis tends to be only on 24h basis providing water scenario, energy scenario and water-energy nexus scenario separately. A MILP optimization model for wind-powered desalination units, where the number and type of turbines are optimized based on technical and economic factors is presented in [27]. The model includes the integration of a diesel generator, BES, and a water storage tank to reduce costs and improve reliability. Approach uses both BES capacity and power as variable and uses binary variables for charge and discharge options. However, RES capacities are not variables, but number of RES options. Furthermore, it uses 24h equivalents and not whole year horizon period.

1.2. Desalination and Water-Energy Nexus approach

Remote islands often face freshwater shortages due to limited resources, exacerbated by the seasonality of tourism. Traditionally, many islands relied on transporting water via boats, significantly increasing costs. As a result, desalination has emerged as a cost-effective and sustainable solution to meet freshwater demands efficiently [28].

Islands face energy resource constraints, making energy-intensive desalination a challenge. A sustainable solution is pairing RES with desalination, addressing water shortages while avoiding fossil fuel dependence and ensuring environmental sustainability. The authors in [29] give a detailed review of different desalination and RES technologies focusing mostly on RO desalination. Similarly, the authors in [30] review existing desalination and RES applications, emphasizing energy storage and process optimization for greater efficiency and cost-effectiveness. Detailed overview of the RES integration with a highlight on technical issues, environmental, and economic impact was further shown in [31]. Authors give a more thorough view on technical issues, environmental and economic impact. The authors in [32] tested a stand-alone wind-powered desalination prototype on Gran Canaria, evaluating reverse osmosis, electrodialysis reversal, and vacuum vapor compression. Reverse osmosis proved the most effective for intermittent wind energy, offering stable water quality and efficient operation. The study [33] reviews over a decade of work on RES powered desalination, testing different desalination technologies using wind and solar energy. Findings from pilot projects in the Canary Islands and Africa show the viability of autonomous desalination, highlighting cost and environmental benefits in off-grid areas.

The authors in [34] optimized the design of a stand-alone RO desalination unit for a Greek island using PV, wind, and hydropower, finding it more cost-effective than water transport. For Gran Canaria, [35] examined a RES-powered microgrid for RO, using wind and PV with grid connection and BES, concluding BES was unnecessary. In [36] a hybrid PV-wind-diesel system with BES was modelled for isolated islands, identifying RO as the most cost-effective desalination method. While HOMER software was used stating the optimisation approach, the study indicates a simulation approach for determining the optimal number of PV and wind units. Comprehensive analysis of wind energy-driven desalination projects in the Canary Archipelago, spanning from 1984 to the present was assessed in [37]. Authors in [38] studied the operation of desalination unit using RES with the implementation of BES, grid connection, and smaller internal combustion engines. The authors used HOMER software for optimisation. However, a study is missing the objective function and what is being optimized. The study [39] applied a Pareto front optimization approach with automated EnergyPLAN simulations to determine optimal capacities for water-energy systems on Lanzarote Island. By integrating flexible desalination as a load, the method increases renewable energy contribution from 5.14% to 24.6%, balancing wind and PV capacities, water storage, and desalination to maximize renewables while minimizing CO2 emissions, fossil fuel use, and costs.

Authors in [40] a continuously operated RO model with PV power, BES, and water storage showed that a smaller BES suffices without grid connection. To tackle the problem of higher BES costs that are generally used as a flexibility resource on the energy system side, a study of using only seasonal water storage for PV based RO system is shown in [41]. Even though authors mention optimization, it seems they used brute-force approach to determine the number of PV panels. Study [42] addresses water and energy challenges on Greek islands by developing an optimal desalination systems powered by RES. Although no optimisation approach was used, authors simulate water storage and RES integration.

Authors in [43] propose a method for optimizing island water-energy systems by integrating wind, hydrogen storage, and RO desalination. Optimization aims to minimize the total system cost and was tested on typical summer and winter days for a 24h periods. The study [44] compared PSO and HOMER software for optimizing the sizing and dispatch of PV and hydrogen based RO desalination system. Authors conclude how PSO optimisation approach outperforms HOMER. Although it uses PSO approach, optimal number of model actors is selected, and not optimal value capacities. Iterative "optimization" method for sizing a stand-alone hybrid PV/wind/hydrogen system to power a desalination unit was proposed in [45]. A case study on the Kerkennah islands was proposed. Like other semi-optimisation approaches, it uses iterative simulation approach to find the most cost-effective option for a number of investigated scenarios. Similarly, although mentioning optimisation of water and energy system approach, authors in [46] use iterative "optimization" approach to design power system for RO in remote communities, including Honduras, Eritrea, and Australia.

1.3. Optimisation approaches in Water-Energy system modelling

When studying the literature on desalination and water-energy nexus, even though one can still find a more basic simulation approaches, it is now a common thing to see the optimization approaches being used. It is also common to see authors use the optimization wording relatively "freely", sometimes not stating which optimization approach was used and what was the optimization problem. Hence, below we cover main optimization approaches used in field of water-energy nexus, and more specific the implementation of desalination, RES, storage, and DSM technologies.

The authors in [47] reviewed desalination optimization models, highlighting energy consumption, transport, fouling, and integration with RES. They pointed out that while hybrid desalination technologies show promise, the review lacks detailed optimization discussions. In [48] he authors offer an extensive review of optimization approaches in RES-RO modelling, categorizing methods into classical techniques (e.g., Newton's method, Simplex) and AI-based methods (e.g., Particle Swarm Optimization, Evolutionary Algorithms, Simulated Annealing).

We provide a brief review of recent optimization approaches for desalination, RES, and storage. We classify methods into two main types: those using commercial software and those based on custom models created with coding tools like Python, Matlab, or GAMS. The latter approach allows for transparency in the objective function and constraints, whereas commercial software like HOMER often lacks such detail. Many studies using HOMER, [36], [38], [49], appear to select the optimal scenario based on cost from multiple simulations, rather than a true optimization approach. Similarly, other approaches not related to HOMER, and previously mentioned, tend to mention optimisation while the methods suggest the iterative simulation approach was used [15],[34],[42],[45],[46].

A popular optimization technique seen in literature is the usage of iterative heuristic and meta-heuristic approaches. The authors in [50] put nineteen different heuristic and metaheuristic algorithms to the test to find the optimal RO-RES system. Included RES solutions were wind and PV power while also including a BES. Both the individual and hybrid heuristic and metaheuristic optimization approaches were assessed. The authors conclude that improved harmony search-based chaotic simulated annealing algorithm provided the best results in regards to the mean, min, and max values. Moreover, authors add that hybrid metaheuristic algorithms, the ones combining two or more single optimization approaches, are more superior to individual optimization algorithms due its faster convergence speed and calculation accuracy. Many authors in previously mentioned references use iterative heuristic and meta-heuristic approaches for water-energy system analysis [11],[16],[18],[20],[21],[35],[44]. Iterative heuristic and meta-heuristic approaches can be less efficient than linear programming methods because they often require more computational time to converge and do not guarantee optimal solutions. These methods rely on approximation and trial-and-error processes, which can lead to suboptimal results, whereas linear programming methods offer a systematic approach to find the best solution within given constraints, ensuring optimality and faster convergence. Therefore, a concept of linear programming has grown significantly in popularity during the last several years in the field of water-energy nexus.

In study [51], a MILP model was used to optimize RES dispatch through demand response in the Canary Islands' water supply sector. The results show that demand shifting increases self-sufficiency and RES utilization, with the highest self-sufficiency achieved by combining both PV and wind power. Authors in [52] proposed a MILP-based short-term scheduling approach for desalination unit operation and thermal power unit scheduling. It includes water energy storage and BES integration with power flow constraints. The authors demonstrate that the model significantly reduces system operation costs and recommend its use for future water-energy nexus challenges. Before mentioned studies in sections 1.1 and 1.2 deploy the LP optimisation approach for water-energy system analysis [13],[14],[17], [22],[24],[25],[27].

1.4. Proposed paper contribution

The proposed study presents a comprehensive assessment of water and energy systems through an optimization framework, providing the optimal dispatch of water and energy streams while determining

the optimal capacities for BES and RES. This approach incorporates water storage and PtW technology, offering a novel perspective on integrated water-energy system optimization.

Existing research highlights a gap in the holistic optimization of capacity and dispatch for islanded systems, particularly those experiencing pronounced seasonality.

While some studies focus on detailed optimization of energy systems or storage capacities, they often neglect the integration of water storage and water system optimization. Conversely, studies cantered on water systems rarely include RES or energy storage capacity optimization or extend their analyses to shorter time horizons.

The literature review underscores the absence of a broader optimization framework that simultaneously addresses water and energy system capacities and their operational dispatch, alongside storage solutions. To bridge this gap, this study proposes an innovative implementation of MILP model that optimizes RES and BES capacities, coupled with water systems through RO desalination unit and water storage supported by PtW technology.

Unlike the traditional approach in water-energy system analysis, which often focuses solely on BES capacity optimization, this study adopts a more detailed methodology. Similar to advanced studies [22],[25],[26],[27] the proposed model considers both BES capacity and power rating as variables. It extends this approach by including RES capacity optimization, water system modelling, and water storage integration. Additionally, the model provides an optimized hourly dispatch for RES (primarily PV power), BES, grid connection, and RO desalination for a full one-year period, offering insights into enhanced system flexibility and integration through PtW.

The proposed integrated water-energy system model delivers optimal system capacities and the dispatch of energy and water streams. Notably, the study addresses the unique challenges faced by smaller-scale island systems, which are often overlooked in larger-scale water-energy nexus analyses. These systems are particularly affected by tourism-induced demand fluctuations, which can cause up to tenfold variations in total system demand. By focusing on the Croatian island of Unije as a case study, the research provides valuable insights into island-specific dynamics, with detailed case data presented in Section 3.

Furthermore, the study explores the impact of varying PV and BES investment costs, offering a range of optimal solutions based on different cost scenarios. This analysis provides a comprehensive overview of system operational capacities and economic performance, which can inform practical assessments of water-energy systems in islands and remote areas. Finally, the effects of changes in grid electricity prices, PV potential, and water demand on optimal system configuration and financial outcomes are thoroughly evaluated, making the findings highly relevant for future applications and decision-making in water-energy system design.

1.5. Paper organization

The remainder of the proposed study is divided into: Section 2 where a detailed description of the proposed MILP based water-energy system optimisation model, and modelling framework is presented. The Section 3 follows with clarification on case study, used input data and assumptions for the specific parameters, demand curves, price curves etc. The Section 0 presents a detailed analysis and discussion of the optimal water-energy system configuration for Unije Island, focusing on the joint RES, water and BES storage operation. Additional change in grid electricity price, PV potential, and water demand is shown after base results. Finally, conclusion and future work is provided in the Section 5.

2. Method - Water-energy nexus model

A MILP optimisation approach for optimising integrated water and energy systems is proposed, offering the flexibility to incorporate any water production, treatment, or storage technology, as well as any electricity generation or storage technology, with the inclusion of energy to water system connection.

This model is designed to identify the optimal dispatch of water and energy streams while simultaneously determining the optimal system capacities. The framework is highly adaptable, enabling users to include various technologies depending on specific system requirements, as illustrated in Figure 1.

The model was applied to optimize the dispatch of water and energy system components while determining the optimal sizing of electricity generation technologies, storage power and energy capacities, and key water system parameters.

In the proposed setup, PV generation was selected as a main power source to support the sustainability and study the RES integration. Additionally, a grid connection was incorporated to evaluate the economic implications of RES and storage integration into existing island water-energy system, which traditionally rely heavily on grid connections and/or fossil electricity generation technologies.

To assess the impact of Power-to-Water (PtW) through the operation of a desalination unit, water storage was included as a component of the water-energy system optimization model. Furthermore, to explore the interactions between electricity generation and various storage options, a BES storage system was incorporated, with both its optimal capacity and power values modelled. The sets, variables, and parameters used in the model are comprehensively detailed in Nomenclature.

The modelling framework operates on a yearly time horizon, allowing the user to select a desired time step for their specific application. In this study, an hourly time step was chosen as a balance between achieving high temporal resolution and maintaining reasonable computational efficiency. This selection reflects the trade-offs inherent in optimization models, particularly MILP formulations, which are more computationally intensive than basic LP models and depend heavily on system hardware configurations. However, the framework is flexible, permitting the use of higher-resolution time steps if supported by advanced computational resources.

The optimization problem was implemented in Python 3.7 using the GUROBI solver for mathematical optimization. The GUROBI Python extension module (gurobipy) was installed and integrated into the Python environment to enable efficient execution. All optimizations were performed on a workstation equipped with two Intel Xeon E5-2623 v3 CPUs and 64 GB of RAM, with an average runtime of approximately 30 minutes per optimization run.

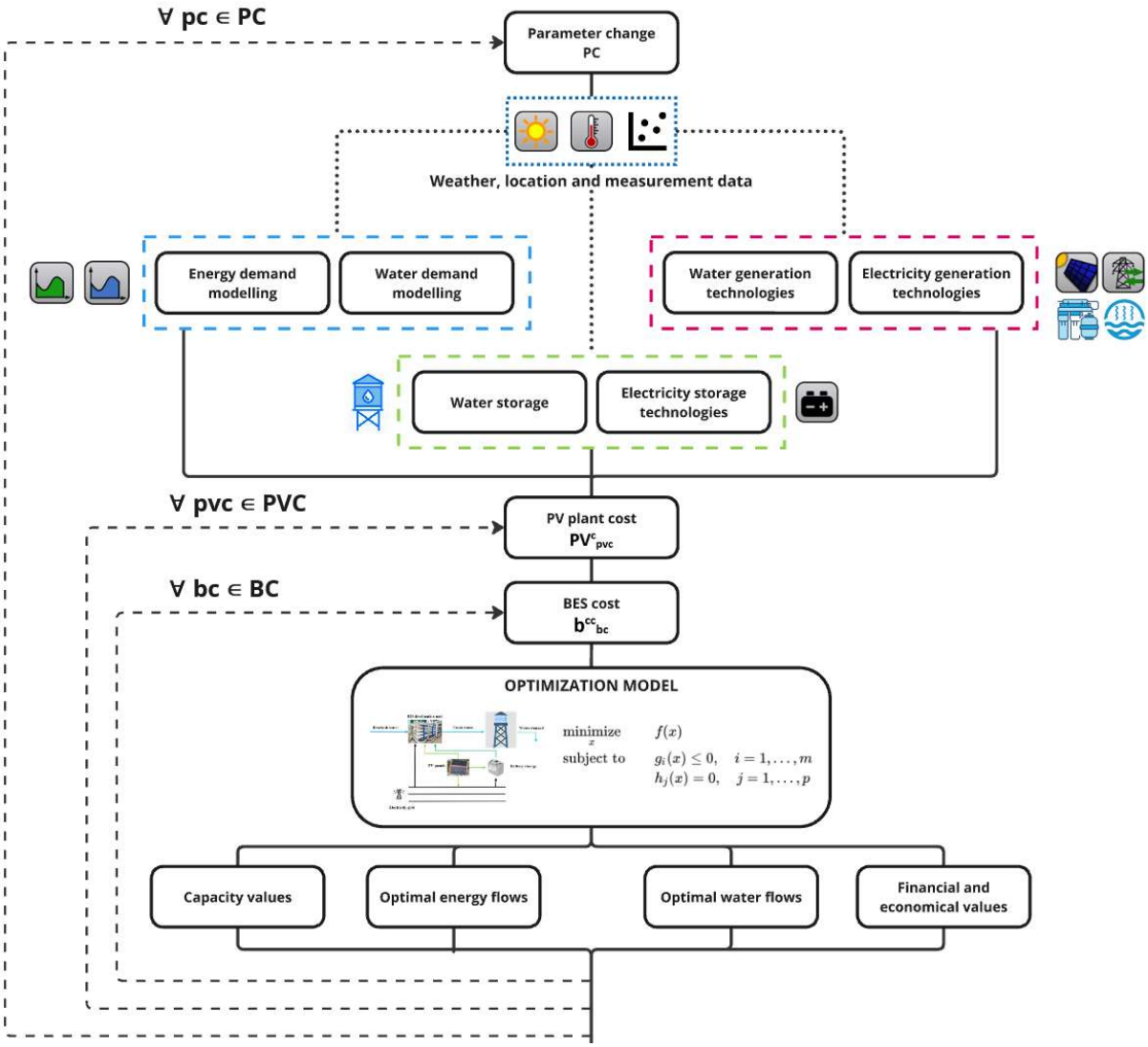


Figure 1. Schematic of the modelling and optimization approach

Figure 1 illustrates the schematic of the proposed modelling and optimization approach, which can be divided into three main sections.

The first section focuses on the selection of system-side technologies and the definition of input parameters along with representative time-series data. This includes identifying water generation and/or treatment technologies and energy system technologies, enclosed within the dashed red rectangle. Additionally, the selection of storage options, encompassing both water and energy storage systems, is highlighted within the dashed green rectangle. Depending on the defined system boundaries, inputs in the form of energy demand and/or water demand may be required. To address this, weather data, site-specific information, and existing measurement datasets are modelled to generate tailored demand profiles, represented within the dashed and dotted blue rectangles.

In the proposed case study, the system boundary encompasses the desalination unit, the associated water pipeline system, and water storage. Consequently, water demand is the primary input, while electricity demand is derived as an output of the optimization process, based on the optimal operation of the desalination unit and the selected PV and energy storage configurations. However, in cases where the system boundary includes broader energy systems, additional energy demand inputs may be necessary, as indicated in the Figure 1.

The second section outlines the optimization approach, which is structured around variations in specific parameters, PV investment cost, and BES investment cost. Changes in specific parameters are represented by the outermost loop, while changes in PV and BES investment costs are captured within two nested inner loops, illustrated with black dashed lines in the schematic.

The outermost loop represents variations in key parameters that significantly influence the optimal configuration and dispatch of the water-energy system. For each parameter change pc within the parameter change set (pc ∈ PC), a set of optimization runs is performed. Each selected parameter itself represents a set of different parameter changes based on which set of optimisation runs is made. Therefore, a set of grid electricity price change ($\varepsilon \in \Omega_E$), set of PV potential change ($\kappa \in \Omega_K$), and set of water demand change ($\psi \in \Omega_\Psi$) was selected as important parameters change.

The second loop corresponds to changes in PV investment cost. For each value pvc within the PV cost set (pvc ∈ PVC), an optimization run is executed. Nested within this loop, the third and innermost loop addresses variations in BES investment cost. For each value bc within the BES investment cost set (bc ∈ BC), an optimization run is initiated. Each run aims to minimize the objective function, ultimately determining the optimal configuration of the water-energy system under the given parameter conditions.

The third section presents the outputs of the proposed framework, including optimal system capacities, time-step-based energy and water flows, and key financial and economic indicators. By performing multiple optimization runs, the framework generates a comprehensive set of results detailing the optimal water-energy system configurations under varying PV and BES investment costs. Additionally, variations in the three key parameters provide insights into the impacts on overall system profitability, optimal renewable energy and storage capacities, and the dispatch of water and energy systems.

An optimisation model objective function and main model constraints are shown below. The first paragraph explains the main objective function and what it is composed of. The following paragraph shows the main constraints regarding the proposed energy system while the last paragraph discusses on the constraints for the water system and its connection to energy system.

The objective function is composed of the sum of the system costs, and potential financial and economical savings which can be seen in equation (1).

$$\begin{aligned}\min \quad & \sum_t e^{P}_t \cdot G^{D}_{pvc,\,bc,\,t} + \sum_t e^{P}_t \cdot B^{CH,G}_{pvc,\,bc,\,t} + \sum_t w^{BC} \cdot W^{B}_{pvc,\,bc,\,t} + \sum_t ll^{c} \cdot LL_{pvc,\,bc,\,t} + \\ & \sum_t pv^{var} \cdot PV^{E}_{pvc,\,bc,\,t} + B^{C}_{pvc,\,bc} \cdot b^{MCC} + B^{NP}_{pvc,\,bc} \cdot b^{MPC} - \sum_t e^{P}_t \cdot PV^{D}_{pvc,\,bc,\,t} - \sum_t e^{S}_t \cdot PV^{G}_{pvc,\,bc,\,t} - \\ & \sum_t e^{P}_t \cdot B^{DC}_{pvc,\,bc,\,t} + B^{C}_{pvc,\,bc} \cdot b^{CC}{}_{bc} \cdot \zeta \cdot cr + B^{NP}_{pvc,\,bc} \cdot b^{PC}{}_{bc} \cdot (1-\zeta) \cdot cr + \\ & PV^{P}_{pvc,\,bc} \cdot pv^{C}{}_{pvc} \cdot cr + B^{C}_{pvc,\,bc} \cdot b^{CC}{}_{bc} \cdot icdf \cdot pvf \cdot \zeta \cdot cr + B^{NP}_{pvc,\,bc} \cdot b^{PC}{}_{bc} \cdot icdf \cdot pvf \cdot (1- \\ & \zeta) \cdot cr, \quad (\forall\, pvc \in PVC, \forall\, bc \in BC, \forall\, t \in T)\end{aligned} \tag{1}$$

The objective function of the proposed problem is to minimize the total system cost on the annual basis. It encompasses several components, each representing a specific cost or saving within the system. These components can be categorized as follows:

- Grid electricity cost - the grid electricity cost is a significant component of the objective function. It is composed of two terms where the first one represents the cost of grid electricity required for running the desalination unit, while the second term represents the cumulative cost of grid electricity used for charging the BES. These costs directly impact the operational expenses of the system, and are shown as the first two summations in the equation 1,
- Cost of water boat carriers - in situations where the desalination unit cannot produce sufficient fresh water to meet the demand, water boat carriers are utilized. This component in the objective function represents the cost associated with employing water boat carriers for the transportation of water. It captures the expenses incurred when alternative means are required to fulfil the water demand. The water boat carriers in optimisation approach can also be seen as a loss of load on a water supply side,
- Lost load cost - the objective function includes a term that represents the lost load cost for electricity production. This cost arises when the system is unable to meet the electricity demand,

resulting in a loss of potential revenue. By considering this cost, the objective function accounts for the economic consequences of insufficient electricity production,

- Variable cost of PV electricity generation - the objective function incorporates a term that represents the variable cost associated with using PV for electricity generation. This component includes expenses related to the maintenance, operation, and other variable costs specific for the PV technology,
- BES maintenance cost
- Financial and economical savings - the summations with negative signs represent the financial or economical savings generated by the system operation. These savings can be further divided into savings due to the direct PV usage for desalination purposes, earnings from excess PV generation sold to the grid, and savings due to BES usage, respectively seen as a negative summation in the equation 1,
- Annualized investment cost - reflects the expenses incurred for the initial setup, installation, and financing of these renewable energy components. It is worth noting that the general approach of using only BES capacity as the variable in the objective function is here further divided into the battery storage capacity in kWh, and nominal BES power kW where ζ represents the weighting factor for the two battery storage costs. The base case value for the ζ is 0.5,
- Annualized BES replacement cost – reflects the annualised expenses for the replacement of BES in year *ry.* Factor *icdf* represents the BES investment cost decrease factor for a year *ry,* while present value factor *pvf* determines the present value of the future BES replacement cost.

Model is additionally constrained by the equations and inequalities (2)-(28) that are simulating the physical energy and water flows, as well as the physical boundaries for the water-energy system operation based on the RES and BES. Below are the main constraints regarding the energy system side.

Equation (2) represents the demand-supply balance where on the LHS of the equation are energy input variables such as PV generation, BES discharge and grid connection, while the RHS of the equation is composed of the electricity demand and lost load variables.

$$PV^{D}_{pc,\,pvc,\,bc,\,t} + B^{DC}_{pc,\,pvc,\,bc,\,t} + G^{D}_{pc,\,pvc,\,bc,\,t} = E^{D}_{pc,\,pvc,\,bc,\,t} - LL_{pc,\,pvc,\,bc,\,t}, \quad (\forall\, pvc \in PVC, \forall\, bc \in BC, \forall\, t \in T) \tag{2}$$

Constraints ranging from (3)-(16) describe the energy system side and specific limitations on BES operation. Equation (3) represents the BES state-of-charge (SOC) for each timestep t ∈ [1, T]. The RHS of the BES SOC equation is composed of the SOC in the previous time step with the inclusion of self-discharge, BES grid and PV charging and charging efficiency, and BES discharge and its corresponding discharge efficiency. Set of constraints from (4)-(7) gives further limits on the BES SOC and capacity. Equation (4) sets the starting SOC in time step t=0 as a percentage of global BES capacity while constraint (5) limits the final SOC in the time step t=T to values higher or equal to the staring BES SOC. To further model BES operation in a sense of capacity preservation, equations (6) and (7) limit the lower and upper usable BES capacity. As model differentiates BES power and capacity, further limitations on BES nominal power output are shown in constraints (8)-(11).

Constraints (8) and (9) represent the upper and lower limits on the time-step based power output, respectively. Global nominal BES power output is the upper limit for the time-step based power output values and shown in the constraint (10). Similarly, constraint (11) limits that time-step based power output is lower than the global nominal BES capacity.

$$B^{SOC}_{pvc,\,bc,\,t} = B^{SOC}_{pvc,\,bc,\,t-1}\cdot(1-b^{sd}) + (B^{CH,G}_{pvc,\,bc,\,t} + B^{CH,PV}_{pvc,\,bc,\,t})\cdot b^{ch,\eta} - {B^{DC}_{pvc,\,bc,\,t}}/{b^{dc,\eta}}, \quad (\forall\, pvc \in PVC, \forall\, bc \in BC, \forall\, t \in [1, T]) \tag{3}$$

$$B^{SOC}_{pvc,\,bc,\,t} = b^{SOC}_{t0}\cdot B^{C}_{pvc,\,bc}, \quad (\forall\, pvc \in PVC, \forall\, bc \in BC, t = 0) \tag{4}$$

$$B^{SOC}_{pvc,\,bc,\,t} \geq b^{SOC}_{t0} \cdot B^{C}_{pvc,\,bc}, \quad (\forall\, pvc \in PVC, \forall\, bc \in BC, t = T) \tag{5}$$

$$B^{C}_{pvc,\,bc} \cdot b^{SOC,max} \geq B^{SOC}_{pvc,\,bc,\,t}, \quad (\forall\, pvc \in PVC, \forall\, bc \in BC, \forall\, t \in T) \tag{6}$$

$$B^{C}_{pvc,\,bc} \cdot b^{SOC,min} \leq B^{SOC}_{pvc,\,bc,\,t}, \quad (\forall\, pvc \in PVC, \forall\, bc \in BC, \forall\, t \in T) \tag{7}$$

$$B^{P}_{pvc,\,bc,\,t} \leq b^{P,max}, \quad (\forall\, pvc \in PVC, \forall\, bc \in BC, \forall\, t \in T) \tag{8}$$

$$B^{P}_{pvc,\,bc,\,t} \geq b^{P,min}, \quad (\forall\, pvc \in PVC, \forall\, bc \in BC, \forall\, t \in T) \tag{9}$$

$$B^{NP}_{pvc,\,bc} \geq B^{P}_{pvc,\,bc,\,t}, \quad (\forall\, pvc \in PVC, \forall\, bc \in BC, \forall\, t \in T) \tag{10}$$

$$B^{C}_{pvc,\,bc} \geq B^{P}_{pvc,\,bc,\,t}, \quad (\forall\, pvc \in PVC, \forall\, bc \in BC, \forall\, t \in T) \tag{11}$$

Further constraints ranging from (12)-(14) show the connection between the time-step based BES power output/input and its energy equivalent for selected time-step Δt. X variables are binary variables limiting that only one operation, either BES charging or discharging, can be done in one time-step and it is shown in constraints (15) and (16). The abovementioned constrains are adding mixed-integer part in the linear programming problem. Furthermore, one can see that multiplication of variables sets this problem as quadratic, and not linear. Hence, this model can be expressed as MIQCP problem. Even though the GUROBI solver, which was used for this study, automatically does linearization of multiplication of two variables, additional linearization of constraints (12)-(14) can be done using upper and lower BES power limits per common linearization technique [53], making a problem MILP.

$$B^{CH,PV}_{pvc,\,bc,\,t} \leq B^{P}_{pvc,\,bc,\,t} \cdot \Delta t \cdot X^{PV}_{pvc,\,bc,\,t}, \quad (\forall\, pvc \in PVC, \forall\, bc \in BC, \forall\, t \in T) \tag{12}$$

$$B^{CH,G}_{pvc,\,bc,\,t} \leq B^{P}_{pvc,\,bc,\,t} \cdot \Delta t \cdot X^{G}_{pvc,\,bc,\,t}, \quad (\forall\, pvc \in PVC, \forall\, bc \in BC, \forall\, t \in T) \tag{13}$$

$$B^{DC}_{pvc,\,bc,\,t} \leq B^{P}_{pvc,\,bc,\,t} \cdot \Delta t \cdot X^{DC}_{pvc,\,bc,\,t}, \quad (\forall\, pvc \in PVC, \forall\, bc \in BC, \forall\, t \in T) \tag{14}$$

$$X^{PV}_{pvc,\,bc,\,t} + X^{DC}_{pvc,\,bc,\,t} \leq 1, \quad (\forall\, pvc \in PVC, \forall\, bc \in BC, \forall\, t \in T) \tag{15}$$

$$X^{G}_{pvc,\,bc,\,t} + X^{DC}_{pvc,\,bc,\,t} \leq 1, \quad (\forall\, pvc \in PVC, \forall\, bc \in BC, \forall\, t \in T) \tag{16}$$

Limitations and energy flows regarding the PV generation are shown in constraints (17)-(21). Equation (17) shows that energy generated from PV can be used for direct energy consumption, BES charging or be sold to the grid. Equation (18) shows a simple PV generation form through the usage of PV potential parameter $pv^{S}_{\kappa,t}$ in kWh/kW. The approach of open-source EHDO tool authors for PV generation was used [54]. The *solar_modelling.py* script uses data such as location, elevation, azimuth, weather data, PV module data etc. to find the time-step based PV potential and can be accessed on EHDO Github page [55]. The dependence between the nominal BES power cost and nominal BES capacity cost is shown in the equation (19) where the base value of 0.5 vas used. Equations (20) and (21) represent the grid electricity price curve and selling electricity price curve, respectively. The connection between the grid electricity price and selling electricity price is determined by the parameter γ, often recognised as buy-back factor.

$$PV^{D}_{pvc,\,bc,\,t} + B^{CH,PV}_{pvc,\,bc,\,t} + PV^{G}_{pvc,\,bc,\,t} = PV^{E}_{pvc,\,bc,\,t}, \quad (\forall\, pvc \in PVC, \forall\, bc \in BC, \forall\, t \in T) \tag{17}$$

$$PV^{E}_{pvc,\,bc,\,t} = PV^{P}_{pvc,\,bc,\,t} \cdot pv^{S}_{t}, \quad (\forall\, pvc \in PVC, \forall\, bc \in BC, \forall\, t \in T) \tag{18}$$

$$b^{PC}_{bc} = {}^{b^{CC}_{bc}}\!/_{r}, \quad (\forall\, bc \in BC) \tag{19}$$

$$e^{P}_{t} = e^{P}_{t} \cdot \varepsilon, \quad (\forall\, t \in T) \tag{20}$$

$$e^{S}_{t} = e^{P}_{t} \cdot \gamma, \quad (\forall\, t \in T) \tag{21}$$

Constraints on water system side are shown in set of equations ranging from (22) to (28). Equation (22) represents the water storage level for each timestep t ∈ [1, T]. The RHS of the water storage level is composed of the previous time step water level, addition of water production and water boat carriers' coverage, and subtracted by the water demand. The water production in proposed model is limited only to the water desalination, but further model development will include the other water production technologies to have wider water production possibilities similar to the energy system side.

Set of equations (23)-(26) further limit the water storage operation similarly to the energy system side for the BES SOC constraints. Equation (23) sets the starting water storage level in time step t=0 as a percentage of available water storage capacity while constraint (24) limits final water storage level, in the time step t=T, to values higher or equal to the staring water storage level. Further limitations shown in equations (25) and (26) limit the water storage level between the maximum and minimum values, respectively. Connection between the water and energy system can be observed in the equation (27) where electricity demand is dependent on water production and water production efficiency. The base water production efficiency is generally technology dependent, and here only the water desalination technology is being used. However, the model can include multiple water production and treatment options. Similar to connection between the time-step based BES power output/input and its energy equivalent, the equation (28) limits that the water production in time-step Δt cannot be higher than the installed water production technology generally displayed in m^3/h multiplied by the time-step Δt.

$$W^{L}_{pvc,\,bc,\,t} = W^{L}_{pvc,\,bc,\,t-1} + W^{D}_{pvc,\,bc,\,t} + W^{B}_{pvc,\,bc,\,t} - w^{D}_{t}, \quad (\forall\, pvc \in PVC, \forall\, bc \in BC, \forall\, t \in [1, T]) \tag{22}$$

$$W^{L}_{pvc,\,bc,\,t} = w^{LC} \cdot w^{L}_{t0}, \quad (\forall\, pvc \in PVC, \forall\, bc \in BC, t = 0) \tag{23}$$

$$W^{L}_{pvc,\,bc,\,t} \geq w^{LC} \cdot w^{L}_{t0}, \quad (\forall\, pvc \in PVC, \forall\, bc \in BC, t = T) \tag{24}$$

$$W^{L}_{pvc,\,bc,\,t} \leq w^{LC} \cdot w^{L,max}, \quad (\forall\, pvc \in PVC, \forall\, bc \in BC, \forall\, t \in T) \tag{25}$$

$$W^{L}_{pvc,\,bc,\,t} \geq w^{LC} \cdot w^{L,min}, \quad (\forall\, pvc \in PVC, \forall\, bc \in BC, \forall\, t \in T) \tag{26}$$

$$E^{D}_{pvc,\,bc,\,t} = W^{D}_{pvc,\,bc,\,t} \cdot d^{\eta}, \quad (\forall\, pvc \in PVC, \forall\, bc \in BC, \forall\, t \in T) \tag{27}$$

$$d^{C} \cdot \Delta t \geq W^{D}_{pvc,\,bc,\,t}, \quad (\forall\, pvc \in PVC, \forall\, bc \in BC, \forall\, t \in T) \tag{28}$$

3. Case study: Unije Island

The Unije island is a small island located in the northern part of the Adriatic Sea, part of the larger Cres-Lošinj archipelago, Croatia. The total island area is 16.77 km^2, with a 36.6 km long indented coast. Based on the 2021 census, Unije has 35 private households with 66 permanent inhabitants, while the total number of people in the summer months can rise up to 500 numbering total households to 439 [56].

The population has notable seasonal fluctuations, with an increase in numbers during the summer months brought on by the influx of tourists. This demographic pattern is representative of more general trends seen in many Adriatic islands, where aging and depopulation coexist with sporadic spikes in population brought on by tourism. The weather in Unije is Mediterranean, with hot, dry summers and warm, rainy winters. The climate of the island is suitable for a range of agricultural activities, especially for the cultivation of olives, grapes, and other commodities that are essential to the regional economy. The typical monthly average temperature varies from 7.8 °C in January to 24.6 °C in August, with an annual mean temperature of about 15.3 °C. The island experiences approximately 900 mm of precipitation on average per year, most of which falls in the fall and early winter, in line with the Mediterranean climate [57].

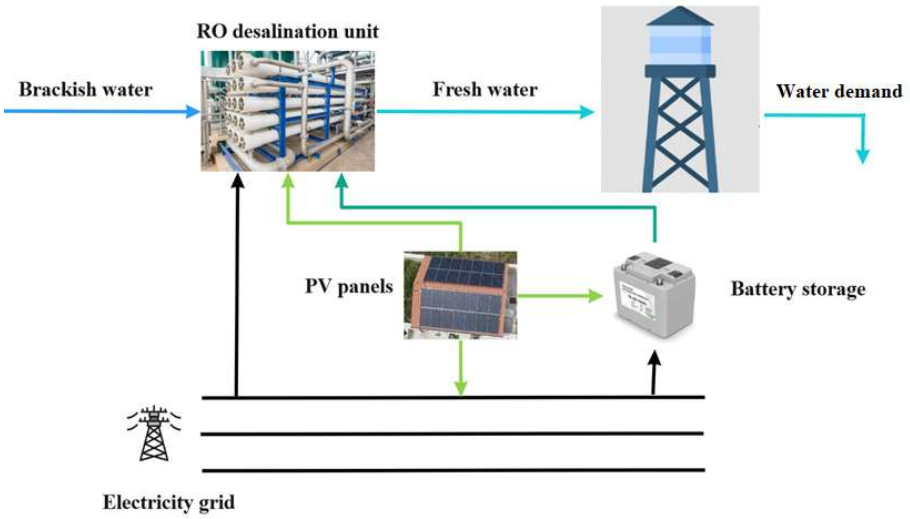


Figure 2. Schematics of water-energy flows for the Unije Island case study

Figure 2 provides a schematic representation of the modelled water-energy system on Unije Island. The water system consists of a RO desalination unit, a water pipeline network, and a primary water storage tank. The energy system includes a PV plant, BES storage and a grid connection. The desalination unit utilizes brackish water from the local aquifer, resulting in an overall energy consumption of 2.5 kWh/m³. The existing water storage tank has a capacity of 400 m³. Hourly water demand data, obtained from the local water utility, is presented in Figure 3. Besides the water hourly demand values, Figure 3 is showing data on number of people on the island and the air temperature values giving the view on the island seasonality and tourism effect. Additional parameter values related to the water system side can be seen in the Table 1.

Table 1. Water system input parameters

Water system input parameters	Model parameter name	Value	Unit
Desalination unit specific consumption	d^{η}	2.5	kWh/m^3
Desalination unit nominal capacity	d^{c}	200	m^3/day
Total water demand	w^{D}_{t}	15939.82	m^3/a
Water storage capacity	w^{LC}	400	m^3
Starting water level	w^{L}_{t0}	40%	% of WS
Max water level	$w^{L,max}$	100%	% of WS
Min water level	$w^{L,min}$	20%	% of WS
Water boat carrier cost	w^{BC}	25	EUR/m^3

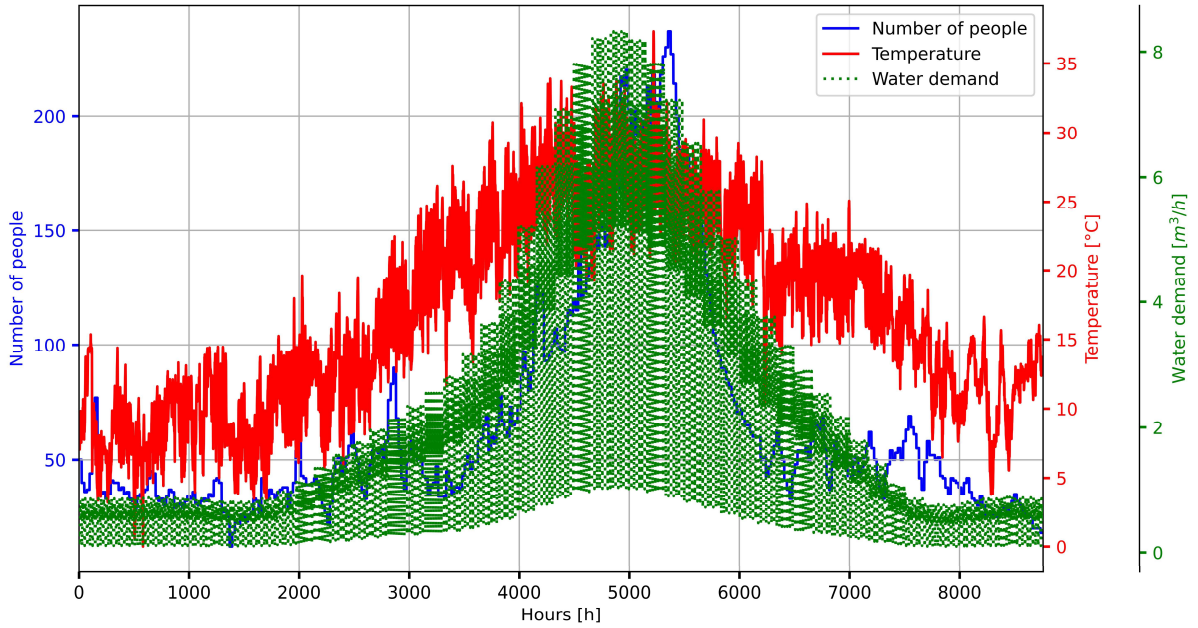


Figure 3. Input data curves for Unije Island

In Croatia, most electricity consumers use a two-tariff pricing model, which was adopted in this study. However, the framework is flexible and can accommodate any electricity price curve. A higher daytime tariff of 130 EUR/MWh was applied between 7 a.m. and 9 p.m., while a lower nighttime tariff of 60 EUR/MWh was applied from 9 p.m. to 7 a.m. The electricity price curve also accounted for daylight saving time adjustments.

To distinguish between electricity purchase and sale prices, a buyback parameter (γ) was introduced. For the Croatian case, any excess electricity sold back to the grid, rather than used for self-consumption, is multiplied by a buyback rate of 0.4. This implies that 60% of potential savings are lost for every kWh sold back to the grid instead of being utilized for self-consumption.

As outlined in Section 2, the methodology for calculating hourly PV generation potential in kWh/kW was adopted from the approach presented by the authors in [54]. The PV investment cost was treated as a variable parameter, reflecting the current market conditions and actual investment costs relevant to the Croatian context. Specifically, with average PV investment costs in Croatia ranging between 1100 and 1200 EUR/kW, the selected range extended from a minimum of 900 EUR/kW to a maximum of 1400 EUR/kW. Additionally, the NREL report [58] was referenced to determine the variable cost of PV power generation, which was calculated as 7.61 EUR/MWh.

Similarly to the PV investment cost range, the BES investment cost range was determined based on current market conditions and real-world investment costs specific to Croatia. As there are only a few existing BES projects in Croatia, available data indicate that BES capacity investment costs remain relatively high, averaging between 500 and 600 EUR/kWh. However, given global trends and the ongoing decline in BES costs, it was assumed that these costs would continue to decrease. Consequently, the selected range spans from a minimum investment cost of 50 EUR/kWh to a maximum of 600 EUR/kWh. Based on this defined BES capacity cost range and the parameter *r,* representing the ratio of BES capacity cost to BES power cost, the BES power investment cost was calculated. To calculate future investment cost for BES replacement, a NREL report [59] was used. A mid-cost decrease projection for BES investment was used resulting with the investment cost decrease factor *icdf* of 0.6. Additional input parameters related to BES utilization are provided in Table 2.

Table 2. BES usage input parameters

BES usage input parameters	Model parameter name	Value	Unit
Minimum BES power output	$b^{P,\,min}$	0	kW
Minimum BES power output	$b^{P,\,max}$	25	kW
BES charge efficiency	$b^{ch,\eta}$	90%	-
BES discharge efficiency	$b^{dc,\eta}$	90%	-
BES self-discharge rate	b^{sd}	1%	% of BES capacity per Month
BES starting SOC	$b^{soc}{}_{t0}$	50%	% of BES capacity
Minimum BES SOC	$b^{soc,\,min}$	20%	% of BES capacity
Maximum BES SOC	$b^{soc,\,max}$	100%	% of BES capacity
BES capacity maintenance cost	b^{MCC}	0.38	EUR/kWh/a [27]
BES power maintenance cost	b^{MPC}	3.22	EUR/kW/a [27]

Annualization of investment cost are with the life-time of technology of 25 years, and the average financial discount rate of 5%. It was assumed that BES replacement is needed in 12^{th} year of studied 25 years project life-time.

4. Results and discussion

The below section present a detailed analysis of the optimal water-energy system configuration for Unije Island, focusing on the joint PV and storage operation. The study examines how variations in PV and BES investment costs influence the system's operational capacities and its overall financial and economic performance. Through a series of optimization runs, the analysis provides insights into the optimal system operation under different cost scenarios, represented by 3D diagrams that map the relationships between PV power, BES storage, and investment costs. The below results and discussion explores how the optimal PV power values change in response to different BES and PV investment costs.

The analysis explores the influence of BES on system performance, emphasizing how variations in BES capacity affect the optimal PV power and the corresponding objective function values, which reflect the system's financial and economic outcomes. Additionally, the study examines BES utilization and its role in enhancing system efficiency, focusing on the interplay between BES power and capacity and their collective impact on storage utilization and overall system savings. This includes a detailed assessment of how BES capacity affects the required BES power and how these parameters together optimize energy storage performance.

The findings further highlight the broader implications for adopting renewable energy and storage solutions, particularly in regions like Unije Island, where seasonal variability significantly impacts energy and water demand. Finally, additional analysis was conducted to evaluate the impact of key parameter changes on the optimal configuration and economic profitability of the future water-energy system on the Unije island. Parameter change analysis systematically varied critical parameters, such as grid electricity price, PV potential, and water demand, to assess their effects on system capacities, dispatch, and overall economic performance. This analysis lays the groundwork for further discussions on the integration of renewable energy sources and storage technologies in contexts characterized by dynamic energy and resource demands.

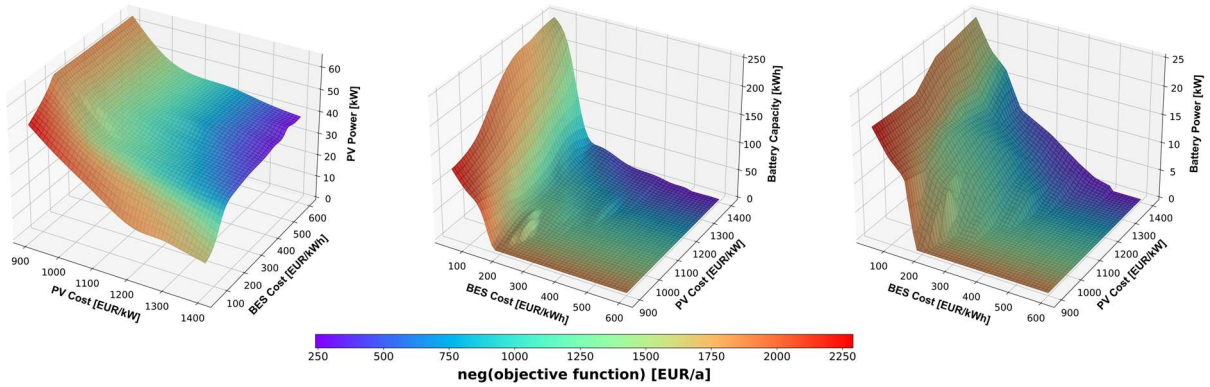


Figure 4. Range of optimal base case capacity results for Unije Island's water-energy system; PV power (left); BES capacity (middle); BES power (right)

The Figure 4 is showing main capacity results regarding the optimal water-energy system for the Unije Island case study. Each of the point is representing the optimal system operation based on the different PV and BES investment costs which are shown as x and y axes. Hence, the shown 3D diagrams are set of multiple optimization runs for different PV and BES investment costs. All shown results depict the optimal system values.

The objective function is composed of the sum of the system costs, and potential financial and economical savings. As the goal is to minimize the objective function, system costs in the objective function are represented with the plus sign while financial and economic revenues are represented with the negative sign. Therefore, if project is to be profitable, final objective function should be below zero. To make it easier for results representation and avoid negative objective function ranges, we display the negative of objective function (*neg(objective function)*) in the results. Therefore, when the overall system is profitable the *neg(objective function)* will be above zero, while for the ones not profitable will be below zero. In a sense, we display the final profitability indicator as negative of objective function that can be seen in equation (1). In the below results, all surface results will be coloured based on *the neg(objective function)* showing that optimal results for different investment cost pairs that are higher than zero as profitable, and those below zero as not profitable. Furthermore, in below results whenever a PV/BES investment cost pair is referenced in numbers, to maintain clarity, units may be not mentioned. However, whenever a PV/BES investment cost pair is mentioned it references the PV cost in EUR/kW and BES investment cost in EUR/kWh.

One of the main points of proposed research was to see the effect of investment cost change on optimal system values. Furthermore, the important part of the research was to study the effect of storage options, here BES and water storage, on RES implementation and total financial and economical profitability. The first diagram on Figure 4 presents the optimal PV power values across the range of selected PV and BES investment costs. As anticipated, lower PV investment costs correspond to higher optimal PV power capacities. However, the rate of change in PV power capacities exhibits notable variability depending on changes in PV and BES investment costs. For instance, when analysing PV power values at a fixed PV investment cost, it becomes evident that the rate of change in PV power is not uniform but is influenced by the associated BES investment cost. One can observe how PV power value rises with higher average rate of 0.124 kW per EUR/kWh for lower BES investment cost values and smooths out to average rate of 0.049 kW per EUR/kWh when approaching higher BES investment costs. In contrast, when observing PV power values for constant BES investment cost, one can observe that rate change is higher for BES cost values up to 200 EUR/kWh with the average rate decrease of -0.069 kW per EUR/kW increase in PV investment cost. Above the 200 EUR/kWh BES cost threshold, the PV

power rate change is lower with average rate decrease of -0.055 kW per EUR/kW increase in PV investment cost. These results are closely tied to BES usage and the second diagram showing the BES capacity in kWh dependent on the PV and BES investment cost.

It is important to note that the axes for “PV cost” and “BES cost” have been switched in the diagrams for clarity and ease of interpretation. A comparison of the first two diagrams reveals that the rate of change in PV power values is strongly influenced by the corresponding BES capacities. Specifically, a higher rate of decrease in PV power is inversely related to a sharp increase in optimal BES capacities when observing changes at a constant PV investment cost.

This relationship underscores that optimal PV and BES configurations exist where PV power serves as the primary energy producer, maximizing direct usage for desalination in a form PtW storage and storage in the form of BES. Consequently, a decrease in optimal PV power is often accompanied by an increase in BES storage, leading to higher *neg(objective function)* values. This observation challenges the common assumption that lower BES costs, and consequently higher BES capacities, always result in greater RES implementation. Instead, the findings suggest that from an optimization perspective, the most effective PV and BES pair does not necessarily maximize both capacities but achieves the best economic outcome as defined by the objective function.

The common conclusion is still relevant, but it is important to define the objective function which determines the optimal value pairs. Further analysis on financial and economical savings will be discussed further below, and are shown in Figure 7 and Figure 8. It is also relevant to notice that BES usage is justified in broader BES cost range with the increase in PV investment cost. However, it is worth noting that those PV and BES pairs result with quite low *neg(objective function)* values of around 500 EUR/a.

The third diagram in Figure 4 illustrates the relationship between BES nominal power and PV and BES investment costs. The BES nominal power results closely follow the trends observed in the BES capacity plane, with notable differences characterized by a higher rate of change at increased PV investment costs. This elevated rate of change is attributed to the continued presence of constant PV power, even at higher PV costs. Consequently, the BES nominal power distribution reflects a combination of the PV power and BES capacity planes. Scenarios with higher PV power, in conjunction with existing BES capacities, result in an increased requirement for BES nominal power, highlighting the interdependence between these variables. This relationship underscores the importance of simultaneously considering PV power and BES capacity when evaluating the optimal configuration of BES nominal power in the system.

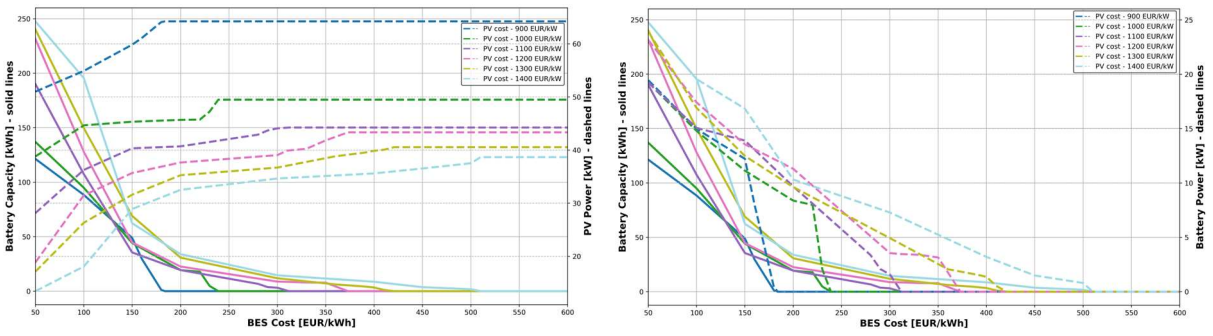


Figure 5. Detailed view on optimal water-energy system capacity values; BES capacity and PV power (left); BES Capacity and BES power (right)

A more detailed analysis of PV power, BES capacity, and BES power is presented in Figure 5. Both diagrams in the figure illustrate results as a function of BES investment costs, displayed along the x-axis. The results are represented as paired solid and dashed lines for each PV investment cost, with each pair distinguished by a consistent colour scheme.

The LHS y-axis in both diagrams corresponds to BES capacity, represented by the solid lines. In the first diagram, the dashed lines indicate PV power values, which are read from the RHS y-axis. Similarly, in the second diagram, the dashed lines represent BES nominal power values, also read from the RHS y-axis. This dual-axis representation provides a comprehensive view of how BES and PV capacities interact across varying BES investment costs, offering insights into their combined impact on system performance and optimization.

The results indicate that higher PV investment costs are associated with a smoother distribution of PV power values, which is directly linked to BES utilization. For lower PV investment costs, the final optimal PV power—represented by the horizontal segments of the dashed lines—is achieved at lower BES cost values. This demonstrates that BES usage becomes more prominent as both PV and BES investment costs increase. Table 3 provides threshold BES cost values below which BES usage is economically justified. In addition to the threshold values, Table 3 also presents the final optimal PV power when BES storage is not utilized and the maximum BES capacities at the lowest BES investment cost. As anticipated, the highest BES utilization occurs at the lowest BES cost of 50 EUR/kWh. However, an intriguing pattern emerges in the BES capacities at this cost. The influence of PV costs on final BES capacity is apparent, and a change from minimum optimal BES capacity of 120.38 kWh to overall maximum BES capacity of 247.60 kWh for PV cost ranges from 900 to 1400 EUR/kW, respectively. These observations highlight the interplay between PV and BES investment costs in determining the optimal capacities, emphasizing the critical role of BES in scenarios with higher investment costs for PV.

Table 3. Overview of base results for ranging PV investment cost – threshold results

PV Cost [EUR/kW]	BES Cost Threshold [EUR/kWh]	PV power w/o BES [kW]	Max BES capacity [kWh]
900	184	64.22	120.38
1000	239	49.48	136.41
1100	312	44.23	189.22
1200	373	43.33	231.49
1300	421	40.54	240.22
1400	510	38.66	247.6

The second diagram in Figure 5, alongside BES capacity, illustrates the BES nominal power values for various PV and BES investment costs. When compared to BES capacity change, we can see that BES power does not have such a high increase in BES power with the increase in PV cost. For example, one can see how BES power at lowest BES cost of 50 EUR/kWh starts with relatively high value of 19.45 kW which is close to the case-study limited power of 25 kW referring the power capacity of the installed desalination unit. With further increase in PV cost, highest BES power is achieved at value of 24.78 kW for PV cost of 1400 EUR/kW.

These findings highlight the necessity of treating BES power and capacity as distinct variables in modelling. In conventional BES modelling approaches that consider only BES capacity, the final optimal BES capacity would likely be underestimated because such models allow charging and discharging to exceed the physical power constraints of the unit. The observed distribution of BES power values, which differ from BES capacity, underscores the importance of explicitly incorporating BES power as an independent variable. This distinction ensures more accurate representation of the physical and operational limits of BES systems, contributing to more reliable optimization results.

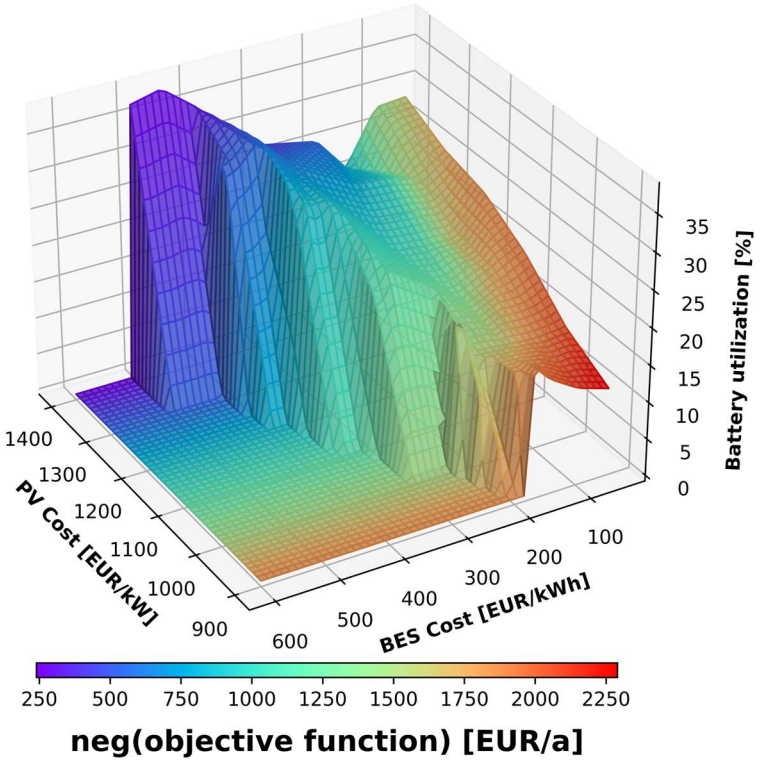


Figure 6. BES utilization parameter

To further evaluate storage utilization and its potential, a BES utilization parameter was developed and is depicted in Figure 6. The BES utilization is defined as the ratio of the energy stored in the BES to the maximum potential energy storage capacity of the BES, calculated on an annual basis and expressed as a percentage. A BES utilization rate of 100% indicates that the storage is being used at full capacity with constant charging and discharging cycles, irrespective of the optimal timing for its operation. While this assumption of full utilization is commonly adopted in research, it does not accurately represent real-world BES operation. The maximum potential energy storage in BES is determined by accounting for both BES power and capacity, under the assumption that every charging cycle is immediately followed by a discharge cycle. This represents the theoretical upper limit of BES cycling potential. Conversely, a BES utilization rate of 0% indicates that the BES is not employed in the optimal system configuration and is effectively excluded from operation. This parameter provides a valuable measure for analysing the role and efficiency of BES in various scenarios and investment cost configurations.

Analysis of BES utilization data reveals an upward trend, where BES utilization increases with higher PV investment costs. This behaviour corresponds to the increase in BES capacity that accompanies higher PV costs. Moreover, it can be concluded that an increase in PV investment cost leads to a shift towards an optimal solution that relies more on BES usage than PV generation, resulting in higher overall BES utilization. In contrast, BES utilization also rises with higher BES investment costs, which seems counterintuitive given the overall decrease in BES capacity. This paradox can be explained by examining the BES power results, where the rate of decline in BES power is smaller than that of BES capacity. Additionally, the highest BES utilization values are observed at threshold BES cost values, where the initial BES usage is economically justified. These optimal solutions typically involve relatively lower BES capacities, which, combined with a smaller rate of decline in BES power, lead to higher BES utilization. Thus, it can be concluded that the highest BES utilization occurs due to a combination of factors: a steeper rate of decline in BES capacity, a smaller decline in BES power, and the influence of lower BES capacity values at the BES cost threshold.

Further important and interesting result is the optimal BES utilization value at the highest *neg(objective function)* point. It is evident that the most profitable optimal solution occurs at the lowest PV and BES investment costs, specifically at a PV cost of 900 EUR/kW and a BES cost of 50 EUR/kWh. This optimal outcome arises from the favourable combination of PV and BES, where PV contributes slightly more to the final solution, while BES serves as storage for excess PV generation, particularly during periods of lower electricity grid tariffs. Moreover, BES utilization exhibits pronounced seasonal behaviour, which is directly tied to the energy and water demand characteristics of the tourist-dependent island of Unije, selected for the case study. Consequently, BES utilization values are expected to be lower, as illustrated in Figure 6, reflecting the system's adaptation to seasonal fluctuations in demand.

As a final remark and discussion starter, one could say that BES utilization results state contradictory conclusions that storage potential is not fully used and has more room for the higher financial and economical savings. However, we would point out reasons why that is not important and what are above results stating. Based on the shown results we state that high BES utilization values are not important for the BES usage justification because the optimization approach gives results that are based on minimisation of objective function which is the sum of all of system costs and potential financial and economical savings. Results are therefore showing that water and energy storage are financially and economically justified for the highly seasonal touristic island and that RES and storage options are jointly taking on the burden of the energy transition. Results of relatively lower BES utilization values for the highest *neg(objective function)* solution shows that there is the optimal PV and BES pair where both take part of the task in providing the financially and economically optimal solution. Therefore, the results are not stating that higher BES capacity are needed at higher PV cost values, but rather that for the optimal energy transition we need both the RES and storage options where with the decrease of investment costs we have optimal combination of RES and storage options that result with the highest financial and economical savings. One could also state that lower BES utilization values go in line with the higher BES lifespan due to the lower numbers of cycles while still achieving the financial and economical benefits. Also worth noting is that provided results do not include external economical benefits such as greenhouse gas emissions savings or health benefits but are to be included in future work expecting that RES and storage options have even higher investment justification.

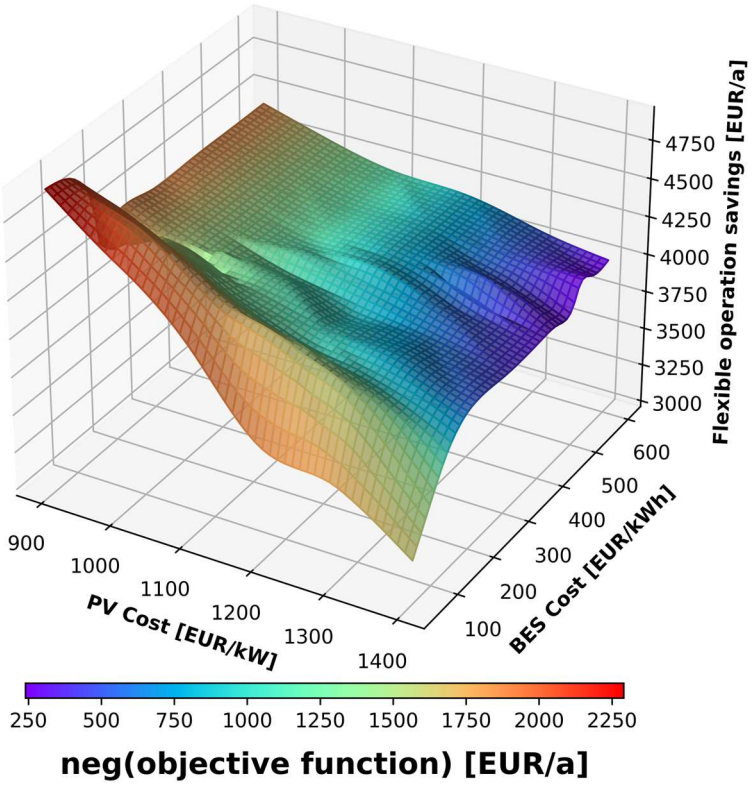


Figure 7. Flexible operation savings

Further below discussion and results follow more closely on financial and economical gains of optimally running water and energy system. Figure 7 is showing the flexible operation savings dependent on different PV and BES investment costs. Flexible operation saving represent a sum of savings due to the usage of storage options. Proposed model differentiates two types of storage options, one being water storage through means of desalination unit (PtW), and BES storage option. Therefore, flexible operation savings represent the sum of savings due to water storage usage where the generated electricity is stored in form of a water for later use, or directly stored in BES. Savings are recognised as any potential difference in RES generated electricity and grid alternative, or the savings due to the electricity tariff difference. To further clarify, any RES generated electricity that is used for the desalination usage, and consequently for water storage, is recognised as a potential saving where the grid electricity price for each time step is used as price alternative. Identical approach for savings due to RES generation being stored in BES was used. The electricity tariff price difference savings can be achieved through means of water or BES storage, where the grid electricity is being used for the desalination usage or BES storage in times of lower tariff, and subsequently used when the grid prices are higher.

Analysing the results in Figure 7, it is evident that the highest flexible operation savings occur at the lowest investment costs for both BES and PV, aligning with the highest *neg(objective function)* point. This behaviour is expected, as higher savings contribute directly to increased *neg(objective function)* values. However, an interesting pattern emerges in the partial fluctuations of overall flexible operation savings as BES capacity increases, which correlates with a reduction in BES investment cost. Since savings are derived from both PtW and BES storage savings, primarily due to PV usage, the main factor differentiating overall flexible operation savings is the specific PV and BES pair combination.

To better understand the behaviour of flexible operation savings, it is crucial to examine the changes in PV power and BES capacity, as shown in Figure 4. When analysing the change in flexible operation savings for a constant PV investment cost, it becomes apparent that the rate of change transitions from a constant decrease in savings at a PV cost of 900 EUR/kW to a constant increase in savings at a PV

cost of 1400 EUR/kW. The continuous decrease and subsequent increase in savings are directly related to the rate changes in PV power and BES capacity. For the 900 EUR/kW PV cost scenario, the increase in PV power is lower than the decrease in BES capacity. This results in a lower increase in PtW storage savings compared to the decrease in BES storage savings, ultimately leading to a reduction in flexible operation savings. In contrast, for a PV cost of 1400 EUR/kW, the higher rate of change for lower BES costs, coupled with the lower rate of change for higher BES costs, results in a positive trend in flexible operation savings.

The primary reason for the lower savings at high PV costs and low BES investment costs is the reduced PV power, which leads to lower PtW storage savings. Despite the highest BES storage savings of 1411.89 EUR/a, aligned with the highest BES capacity, the overall flexible operation savings remain relatively low. As with previous results, it can be concluded that only the optimal combination of both RES and storage yields the highest overall flexible operation savings. When examining the behaviour of flexible operation savings for constant PV costs across the range of investment costs, an interesting pattern emerges. Up to a threshold BES cost of 100 EUR/kWh, there is a rapid increase in savings, followed by a slower decrease in savings. This pattern is directly correlated with changes in PV and BES capacity, influencing the overall savings from RES to water and BES operation.

For constant BES investment costs, the results can be divided into two distinct scenarios. For lower BES costs, savings decrease more rapidly with increasing PV investment costs, which is primarily due to a sharper reduction in PV power compared to the increase in BES capacity. This results in a higher decrease in PtW savings than the increase in BES operation savings. On the other hand, as BES costs rise, the decrease in PV power becomes less pronounced, and the increase in BES capacity slows down, leading to a smaller overall decrease in flexible operation savings.

It is important to note that each data point in the provided results represents the optimal system operation across the entire range of PV and BES investment costs, yielding positive *neg(objective function)* values that state the system profitability. Additionally, when examining flexible operating savings, it is worth mentioning that the absolute difference between the highest and lowest savings is not substantial, amounting to 1676.67 EUR/a. To improve diagram clarity, the z-axis was set to a lower value of 3000 EUR/a. In conclusion, the key takeaway from the flexible system operation savings analysis is that a decrease in both PV and BES investment costs leads to an increase in flexible operation savings, reinforcing the importance of reducing RES and storage investment costs. Furthermore, these results emphasize the critical role of the optimal RES, PtW and BES storage pair, maximizing system performance. Although lower investment costs result in a decrease in optimal PV power and an increase in optimal BES capacity, the overall outcome is the maximization of flexible operation savings, which aligns with the highest *neg(objective function)* values.

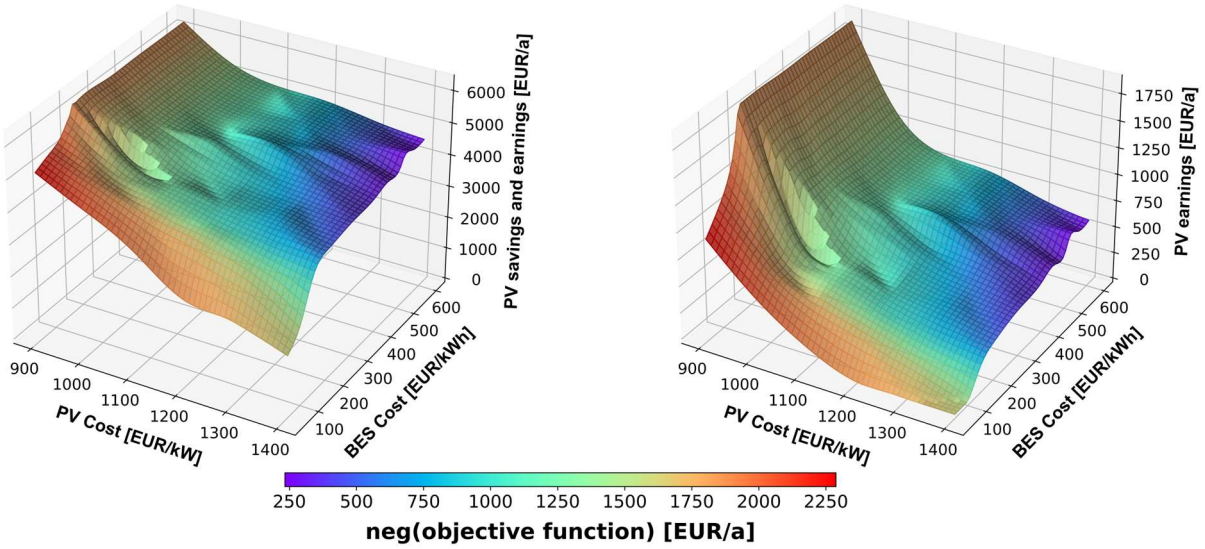


Figure 8. Financial and economical benefits of optimal water-energy system operation; PV savings and earnings (left); PV earnings (right)

Further analysis on financial and economical benefits of optimally running the water and energy system can be seen on Figure 8. Left diagram is showing the sum of savings and earnings due to the PV usage. Similar to flexible operation savings, savings represent economical savings as any potential difference in RES generated electricity and grid alternative. To further clarify, any PV generated electricity that is directly stored in water storage through means of desalination (PtW) is recognised as savings. On the contrary, any excess PV generated electricity that is sold to the grid is recognised as earnings as one directly receives remuneration for that energy stream and can further be seen on second diagram.

By comparing the distribution of PV power in Figure 4 with the first diagram on Figure 8, it is apparent that the PV savings and earnings follow a proportional pattern, with minor variations based on the amount of electricity sold to the grid. The lowest optimal PV power is observed at high PV investment costs and low BES investment costs, which corresponds to the lowest PV savings and earnings at the same investment cost values. As grid electricity is sold at a lower buyback rate, a slight discrepancy between PV power and PV savings and earnings can be observed.

The analysis of PV earnings reveals interesting trends based on different PV and BES investment costs. PV earnings, or the remuneration for electricity sold to the grid, generally follow an increase in PV power. However, the effect of higher BES capacity, driven by a decrease in BES investment costs, becomes evident. As BES investment costs decrease and BES capacity increases, PV earnings begin to drop, eventually reaching zero. This illustrates the relationship between BES capacity and PV earnings, highlighting how increasing BES capacity reduces the need to sell excess PV electricity to the grid.

Table 4. Boundary results for 50 EUR/kWh BES investment cost values

PV investment cost [EUR/kW]	Power to Water Storage		PV to Grid	
	kWh/a	EUR/a	kWh/a	EUR/a
900	32,763.33	4,207.73	17,477.92	908.87
1000	30,232.99	3,892.44	9,475.34	492.49
1100	26,042.44	3,358.26	3,767.93	195.89
1200	19,537.82	2,522.14	214.15	10.98
1300	18,125.28	2,339.15	0	0
1400	14,288.39	1,841.16	0	0

Table 4 presents the values for the boundary BES investment cost of 50 EUR/kWh, where the remuneration for excess PV electricity sold to the grid reaches zero. It is important to highlight that the buyback rate for excess electricity, which varies by country, is a critical parameter influencing the final PV earnings results. Lower buyback rates would likely lead to a scenario where the system favours PtW and BES storage, with zero PV earnings occurring over a broader range of investment costs. Finally, when comparing PV savings and earnings with flexible operation savings in Figure 7, it becomes evident that as BES capacity increases, and consequently BES usage rises, the PV savings and earnings distribution is reshaped into the flexible operation savings distribution. This shift results in the highest savings values being achieved at the lowest investment cost levels, reinforcing the importance of optimizing both PV and BES costs for maximum financial and operational efficiency.

The base results were provided above, and further below we follow with the representation of optimal water-energy system results based on the specific important parameter changes. Three parameters were recognised as important, and range between -30% and +30% change, with 10% step, was selected. Parameters being changed are:

- Grid electricity price - e^P_t
- PV power potential - pv^S_t
- Water demand - w^D_t

To maintain clarity and conciseness, the presentation of optimal capacity results will focus on boundary scenarios, specifically the cases representing -30% and +30% parameter changes.

4.1. Grid electricity price change

Grid electricity price is an important parameter because main revenues (savings and earnings) in provided approach are directly related to equivalent savings (or earnings) in grid electricity prices.

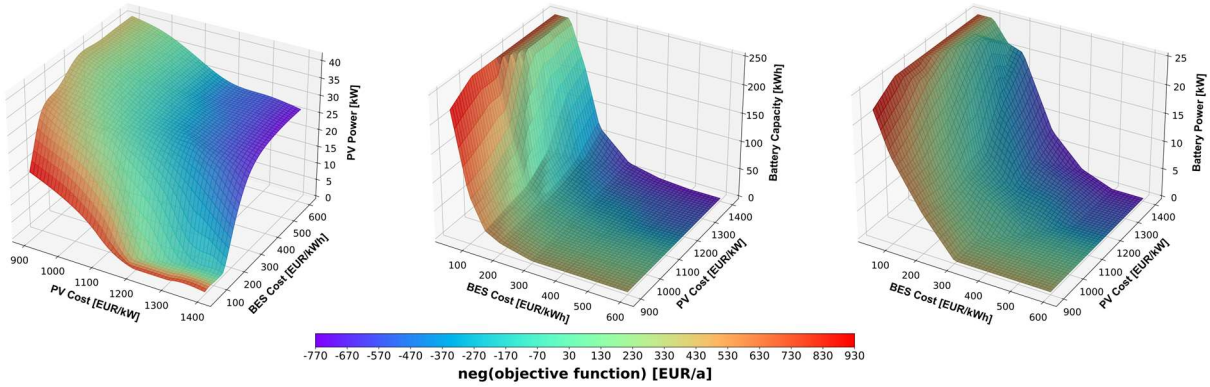


Figure 9. Range of optimal capacity results for Unije Island's water-energy system with 30% decrease in grid electricity price

When comparing the -30% scenario to the base case, the *neg(objective function)* values shift significantly from a range of [240, 2290] EUR/a in the base case to [-770, 930] EUR/a in the -30% scenario. This highlights the substantial impact of grid electricity price changes on the total optimal system capacities and dispatch. It is evident that the highest *neg(objective function)* are achieved at lowest PV/BES investment cost pairs of 900/50. However, the distribution of these highest values (depicted as the red-colored areas in Figure 9) shifts towards regions with lower BES investment costs, indicating that BES storage becomes more dominant in the final optimal solution compared to PV generation and PtW options. Despite this shift, it is important to note that the *neg(objective function)* values in the -30% scenario are still considerably lower than those in the base case, underscoring the reduced financial viability under lower grid electricity prices. Interestingly, the distribution of optimal

PV and BES capacities reveals variability for similar *neg(objective function)* values. For instance, a *neg(objective function)* value of approximately 750 EUR/a (light red area in Figure 9) is achieved at distinctly different investment cost combinations: at 900 EUR/kW for PV and 75 EUR/kWh for BES, and 1400 EUR/kW for PV and 50 EUR/kWh for BES. The respective *neg(objective function)* values for these cases are 776.26 EUR/year and 750.48 EUR/year. These results emphasize the importance of conducting detailed calculations for optimal capacities and dispatch configurations tailored to specific investment cost scenarios. Such analyses are crucial for identifying the most cost-effective solutions, especially under varying grid electricity price conditions.

An additional noteworthy observation is the first occurrence of a non-profitable solution, identified at the investment cost combination of 1100 EUR/kW for PV and 200 EUR/kWh for BES, where the neg(*objective function*) reaches a value of -26.88 EUR/a. Beyond this point, further increases in PV and/or BES investment costs result in increasingly negative neg(*objective function*) values, indicating non-profitability. It is also important to highlight the role of BES storage in maintaining the profitability of the system. For PV investment costs of 1100 EUR/kW and above, BES storage supports profitability within average BES cost ranges below 130 EUR/kWh, as illustrated by the green-coloured areas in Figure 9. This underscores the importance of BES in enabling PV generation and PtW options to remain financially viable under specific investment cost conditions.

From the analysis of optimal capacity values, it is evident that with increasing PV investment costs, PV becomes less viable as an optimal solution at lower BES costs, with BES taking over the entire storage role. This trend is observed in the edge regions of Figure 9, where the optimal PV capacity drops to zero. Specifically, for PV investment costs between 1200 EUR/kW and 1400 EUR/kW, zero PV capacity is seen within BES investment cost ranges of up to 110 EUR/kWh and 170 EUR/kWh, respectively.

A noticeable trend, similar to the base case, is the increase in optimal BES capacity, particularly at higher PV costs. This is evident in Figure 9, where a faster rate of increase in BES capacity is observed as PV costs rise. This phenomenon can be attributed to the higher share of PtW savings and PV earnings at lower PV costs, which diminish as PV costs increase, shifting the reliance on BES to generate greater savings within the total system revenues.

Compared to the base case, optimal BES capacities are generally more prominent, occupying higher values across a broader spectrum of BES investment costs. Conversely, PV capacities are reduced, reflecting a smaller contribution to system savings due to the relatively lower equivalent revenues from grid electricity prices. Notably, the analysis also demonstrates that BES alone can fulfil the role of energy storage, even in the absence of PtW through PV, albeit at significantly lower neg(*objective function*) values. This reinforces the notion that PV and PtW systems are less profitable under these conditions due to lower grid electricity price equivalents.

Furthermore, the reduction in PtW savings and PV earnings results in PV becoming a less competitive solution in the system. However, larger BES capacities compensate to some extent, as they contribute a greater share to total system savings. This increase in BES savings plays a critical role in maintaining profitability, particularly at higher BES capacities, where BES helps offset the diminishing contributions from PV and PtW.

Despite these compensatory effects, it is crucial to emphasize that the final neg(*objective function*) values in the 30% reduction scenario remain significantly lower than those of the base case. This highlights the pivotal role of grid electricity prices in determining the optimal configuration and dispatch of water-energy systems. The results underscore the need for strategic planning to balance the interplay between PV and BES to achieve an economically viable solution under varying electricity price scenarios.

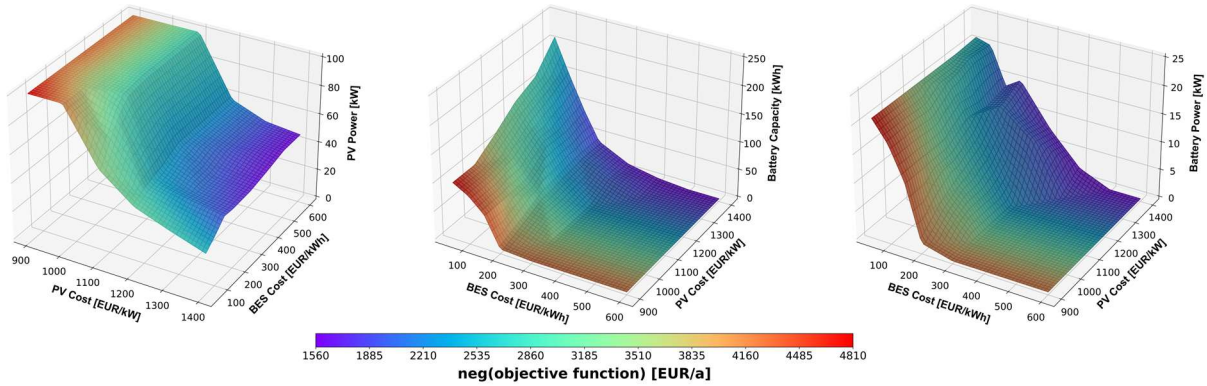


Figure 10. Range of optimal capacity results for Unije Island's water-energy system with 30% increase in grid electricity price

When comparing the +30% scenario to the base case, the *neg(objective function)* values exhibit a significant upward shift, increasing from a range of [240, 2290] EUR/a in the base case to [1560, 4810] EUR/a in the +30% scenario. This highlights the substantial impact of grid electricity price increases on the optimal system configuration and dispatch.

The highest *neg(objective function)* values are observed at the lowest PV and BES investment cost combination of 900 EUR/kW for PV and 50 EUR/kWh for BES. However, in contrast to the scenario with a grid electricity price decrease, the distribution of these highest values (represented as red-colored areas in Figure 10) shifts towards regions with lower PV investment costs. This shift indicates that PtW and PV usage become more dominant in the final optimal solution, while BES options contribute less significantly. This change reflects the increased economic competitiveness of PV and PtW under higher grid electricity prices, as these options provide greater savings and earnings within the overall system.

It is noteworthy that the most profitable solutions per *neg(objective function)* range from 4810 EUR/a for the PV/BES investment cost pair of 900/50 to 4231.54 EUR/a for the pair 900/210, where no BES is deployed. The highest profitability observed in the +30% scenario significantly exceeds the base case, where the maximum *neg(objective function)* reached value of 2290 EUR/a. It is interesting to follow the most profitable base case solution which is on a Figure 10 displayed in blue-teal colours. The closest *neg(objective function)* equal solutions for +30% increase in grid price is seen at PV/BES investment cost pairs of 1200/260 with value of 2280.59 EUR/a when also no BES storage is deployed, at pair 1300/130 with value of 2296.75 EUR/a , and at pair 1400/85 with *neg(objective function)* value of 2292.08 EUR/a. This further confirms that the change in grid electricity cost significantly affects the final optimal arrangement of production capacities and storage options.

The results further reveal that BES contributes less significantly to profitability under the +30% scenario. Instead, PtW and PV usage account for a larger share of revenues due to higher equivalent grid electricity price savings and earnings. Across the PV/BES investment cost range, BES capacities are generally lower compared to the base case. Consequently, BES savings are reduced, but the overall profitability improves as PtW and PV revenues dominate total system revenues.

When examining capacity values, PV deployment reaches its upper limit at lower PV investment costs. Specifically, at PV costs of 900 and 1000 EUR/kW, the PV capacity remains at its maximum irrespective of BES investment costs. At a PV cost of 1100 EUR/kW, maximum PV capacity is achieved for BES investment costs exceeding 220 EUR/kWh, with no BES deployed. For BES costs below 220 EUR/kWh, optimal PV and BES combination is observed, with the PV capacity being below its maximum level but supported by BES storage

Overall, BES appears optimal at slightly lower BES investment costs compared to the base case, as higher grid electricity prices make PtW and PV options more profitable. For the lowest BES cost of 50

EUR/kWh, optimal BES capacities range from 96.73 kWh to 210.90 kWh for PV costs between 900 and 1400 EUR/kW, respectively. On the other hand, PV capacities are higher due to the larger share of savings achieved from the increased grid electricity price. Nonetheless, BES continues to play a role in the optimal system mix, particularly at lower BES costs, generally below 220 EUR/kWh. This demonstrates the complementary relationship between BES and PV in achieving cost-effective solutions, even under scenarios of elevated grid electricity prices.

4.2. PV potential change

PV potential change was recognised as potential critical parameter. As main system revenues are related to PtW and PV generation, below are the optimal system results for the change in PV potential.

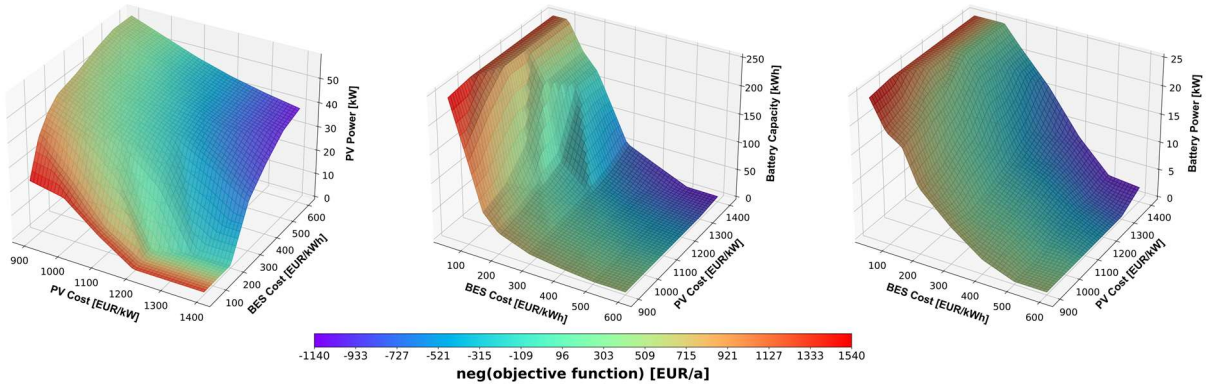


Figure 11. Range of optimal capacity results for Unije Island's water-energy system with 30% decrease in PV potential

Comparing the 30% decrease in PV potential to the base case, the *neg(objective function)* values shift significantly from a range of [240, 2290] EUR/a in the base case to [-1140, 1540] EUR/a in the 30% decrease scenario. Similar to the scenario involving a grid electricity price decrease, this emphasizes the critical impact of PV potential changes on the total optimal system capacities and dispatch. As with the grid electricity price change, a reduction in PV potential causes the distribution of the most profitable systems (depicted as the red-coloured areas in Figure 11) to shift towards regions with lower BES investment costs. This indicates that BES storage becomes more dominant in the final optimal solution compared to PV generation and PtW savings. However, it is important to note that the *neg(objective function)* values in the -30% PV potential decrease scenario are considerably lower than those in the base case, reflecting the diminished economical viability under reduced PV potential.

The 30% decrease in PV potential also reveals variability in the distribution of optimal water-energy system for similar *neg(objective function)* values. For instance, a PV/BES investment cost pair of 900/200 results with a *neg(objective function)* value of 772.61 EUR/a which is by profitability close to *neg(objective function)* value of 764.46 EUR/a seen for investment cost pair of 1400/100. These results further emphasize the importance of conducting detailed calculations for optimal capacities and dispatch configurations tailored to specific investment cost scenarios and identifying the crucial parameters that define the profitability of a water-energy system.

The presence of non-profitable system configurations is also observed in the 30% PV potential decrease scenario. The first occurrence of a non-profitable solution is identified at the investment cost pair of 1100/300, where the *neg(objective function)* reaches a value of -21.30 EUR/a. Beyond this point, further increases in PV and/or BES investment costs result in increasingly negative *neg(objective function)* values, indicating non-profitability. Additionally, for any PV cost equal to or greater than 1100 EUR/kW, configurations where only PV is deployed, and no BES is installed are also non-profitable.

It is worth emphasizing that, across a range of PV and BES investment costs, BES can support system profitability. For PV investment costs equal to or greater than 1100 EUR/kW, BES storage contributes to profitability within a marginal BES investment cost range of 250 to 170 EUR/kWh, corresponding to PV investment costs between 1100 and 1400 EUR/kW, respectively. These areas, depicted in teal colour on Figure 11, demonstrate the crucial role of BES in enabling PV generation and PtW options to remain economically viable under specific cost conditions.

When compared to the 30% decrease in grid electricity prices, it is evident that the impact of a decrease in PV potential is more substantial. The *neg(objective function)* range is wider for both negative and positive values, indicating that decrease in PV potential has a more pronounced influence on system profitability than grid electricity price decrease. This highlights the importance of PV potential in shaping the optimal capacities and annual dispatch.

A noticeable drop in PtW storage is observed under reduced PV potential, as PV becomes less profitable, leading to decreased PtW and PV usage. Conversely, larger BES capacities result in higher BES savings. However, it is crucial to consider that the *neg(objective function)* values are still lower in absolute terms compared to the base case. This can be illustrated by comparing the most profitable case under the 30% PV potential decrease, with a *neg(objective function)* value of 1540 EUR/a, to the green-to-yellow areas in the base case results, as shown in Figure 4. Furthermore, highly negative *neg(objective function)* values confirm that PV potential change is the crucial parameter and these findings further underscore the importance of PV potential in driving the profitability of the system and the critical interplay between PV and BES in achieving optimal water-energy system configurations.

Similar to the scenario of a decrease in grid electricity prices, it is evident that as PV investment costs increase, PV becomes less viable as an optimal solution at lower BES costs, with BES assuming the primary storage role. This trend is observed in the edge regions of Figure 11, where the optimal PV capacity drops to zero. Specifically, for PV investment costs between 1200 EUR/kW and 1400 EUR/kW, zero PV capacity is observed within BES investment cost ranges of up to 140 EUR/kWh and 230 EUR/kWh, respectively. Compared to the grid electricity price decrease scenario, the range of costs where optimal PV capacity equals zero is broader, further indicating that a reduction in PV potential has a more significant impact on the profitability of PtW and PV usage. As the decline in PV potential shifts the system toward greater reliance on BES storage at the expense of PtW and PV usage, higher BES usage is observed across a wider range of PV and BES costs. For instance, even in the boundary case with a PV investment cost of 1400 EUR/kW and a BES investment cost of 600 EUR/kWh, BES is utilized, albeit with a smaller capacity of 4.417 kWh.

As with the base case and the grid price change scenario, the rate of increase in optimal BES capacity varies with specific PV investment costs. This behaviour is apparent in Figure 11, where a faster rate of BES capacity increase is observed at higher PV costs. However, when compared to the base case and the 30% decrease in grid electricity prices, the maximum BES capacity is achieved across a broader range of PV investment costs. For example, for the PV/BES investment cost pair of 900/50, the optimal BES capacity is 243.49 kWh for the 30% decrease in PV potential, 221.73 kWh for the 30% decrease in grid electricity prices, and 121.38 kWh for the base case.

Finally, when compared to the base case and similarly to the grid electricity price decrease scenario, optimal BES capacities are generally more prominent, occupying higher values across a wider spectrum of BES investment costs. Conversely, PV capacities are reduced, reflecting a smaller share of PtW and PV earnings in total system revenues due to the diminished PV potential. Furthermore, the results demonstrate that BES alone can fulfil the role of energy storage even in the absence of PtW through PV, though this occurs at significantly lower *neg(objective function)* values. This highlights the critical role of PV potential decrease in determining the profitability of PtW and PV systems and the complementary role of BES in maintaining system viability under constrained PV conditions.

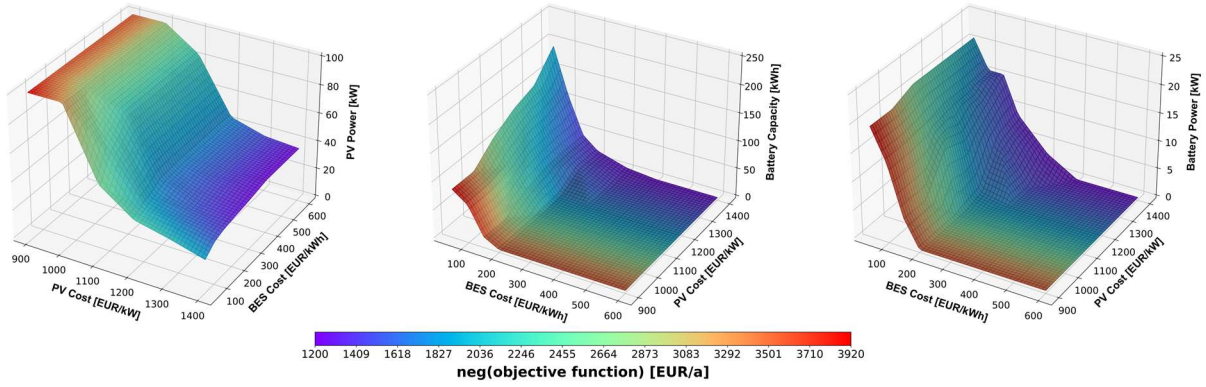


Figure 12. Range of optimal capacity results for Unije Island's water-energy system with 30% increase in PV potential

When comparing the +30% scenario in PV potential to the base case, the *neg(objective function)* values exhibit a significant upward shift, increasing from a range of [240, 2290] EUR/a in the base case to [1200, 3920] EUR/a in the +30% scenario. This highlights the substantial influence of PV potential changes on the optimal system capacities and dispatch. Similar to the 30% increase in grid electricity prices - and in contrast to the scenarios involving decreases in grid electricity price or PV potential - the distribution of the highest values (depicted as the red-coloured areas in Figure 12) shifts towards regions with lower PV investment costs. This shift indicates that PtW and PV generation become more dominant in the final optimal solution compared to BES options.

Notably, the most profitable solution in this scenario, with a *neg(objective function)* value of 3920 EUR/a, is lower than the maximum value achieved in the 30% increase in grid electricity price scenario, which reached 4810 EUR/a. This difference arises primarily due to the upper limit on PV capacity being reached in the PV potential scenario and the slightly higher optimal BES capacities in the grid electricity price increase scenario. The latter scenario benefits from greater PtW and BES savings, driven by higher grid-equivalent savings.

The range of the most profitable solutions in the +30% PV potential scenario spans from a maximum of 3916.46 EUR/a for the 900/50 PV/BES investment cost pair to 3575.31 EUR/a for the 900/170 pair, where no BES is installed. Importantly, the maximum profitability in this scenario exceeds that of the base case, where the highest *neg(objective function)* value is 2290 EUR/a.

It is also insightful to follow the most profitable base case solution, represented in teal colour on Figure 12. The closest *neg(objective function)* values in the +30% PV potential scenario are observed at the PV/BES investment cost pairs of 1100/150 with 2243.62 EUR/a and 1200/50 with 2284.31 EUR/a *neg(objective function)* values. This underscores the significant impact of PV potential changes on the arrangement of optimal production capacities and storage options.

Furthermore, the results indicate that BES has a smaller impact on final profitability in this scenario, as PtW and PV usage contribute a larger share of revenues due to the increased PV potential. However, BES operation and savings are more prominent in the 30% increase in grid electricity price scenario, owing to the higher grid-equivalent savings in that case. In the +30% PV potential scenario, the lower average BES capacities across the PV/BES investment cost range result in reduced BES savings, accounting for just 11.36% of total revenues. Despite this, overall profitability increases due to the greater contribution of PtW and PV earnings, which dominate total system revenues.

Comparing capacity values to the base case, and similar to the grid electricity price increase scenario, PV capacity in the +30% PV potential scenario reaches its upper limit for lower PV investment costs. However, a key difference between the two scenarios is that, under increased PV potential, the maximum PV capacity is achieved only at PV investment costs equal to or below 1000 EUR/kW. In

contrast, for the grid electricity price increase scenario, maximum PV capacity is observed at a PV investment cost of 1200 EUR/kW when BES costs are above 220 EUR/kWh. This broader range of maximum PV capacities and BES storage in the grid electricity price increase scenario results in higher overall profitability compared to the increased PV potential scenario. Across the entire PV/BES investment cost spectrum, BES is cost-effective for BES costs below an average of 170 EUR/kWh. For the lowest BES investment cost of 50 EUR/kWh, the optimal BES capacity ranges from 82.64 kWh to 192.78 kWh as PV investment costs increase from 900 EUR/kW to 1400 EUR/kW, respectively.

Overall, optimal BES capacities are more pronounced at lower levels, as higher PV capacities and the associated PtW savings prove more profitable across a broader range of variable investment costs. The increased PV potential allows PV to operate at higher capacities, generating a larger share of savings due to the enhanced availability of renewable energy. However, BES continues to play a critical role in the optimal system configuration. This demonstrates that while PV becomes increasingly dominant in higher PV potential scenarios, BES retains its importance as a complementary storage solution, especially in cost-effective investment ranges.

4.3. Water demand change

Water demand was recognised as potential critical parameter as it is a main driver for system consumption. Below results show optimal capacity and economic changes based on change in water demand.

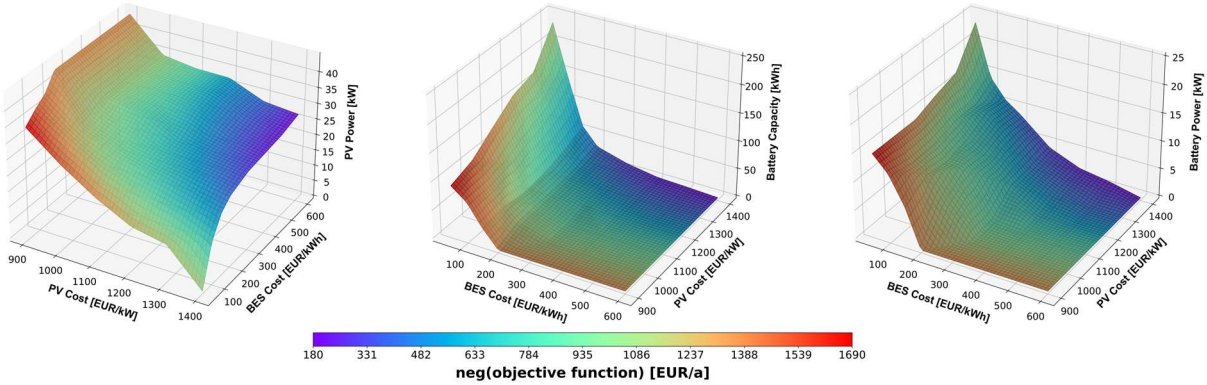


Figure 13. Range of optimal capacity results for Unije Island's water-energy system with 30% decrease in water demand

Comparing the 30% decrease in water demand in Figure 13 to the base case, the *neg(objective function)* values shift from a range of [240, 2290] EUR/a in the base case to [180, 1690] EUR/a in the 30% decrease scenario. This smaller change, compared to scenarios involving grid electricity price and PV potential variations, indicates that reductions in water demand have a relatively lower effect on the overall optimal system configuration and dispatch.

The reduced water demand leads to a greater proportional decrease in revenues from PtW and PV usage compared to savings from BES usage. While both categories experience declines, the impact is more pronounced for PtW and PV savings. Percentagewise, depending on the investment cost pair, BES savings decrease by an average of 14%, whereas PtW and PV savings are approximately 31% lower. In absolute terms, BES savings decrease by an average of 83.50 EUR/a, while PtW and PV usage savings drop by an average of 1378.46 EUR/a.

Following the most profitable solution in the 30% decrease scenario, with a *neg(objective function)* value of 1690 EUR/a, provides additional insights. This solution can be closely compared to its base case counterparts, as represented by the orange-coloured areas in base results Figure 4. In the base case, the closest *neg(objective function)* equal solutions for base case are seen at PV/BES investment cost pairs of 1000/130 with value of 1690.18 EUR/a, at pair 1100/105 with value of 1683.36 EUR/a, at pair

1200/85 with value of 1686 EUR/a, and at pair 1300/60 with 1688.83 EUR/a *neg(objective function)* value.

Overall, the 30% decrease in water demand results in a noticeable decline in revenues from both BES and, PtW and PV usage, with the drop being more significant for PtW and PV savings in both absolute and percentage terms. This is largely due to marginal cases with higher PV costs (≥ 1300 EUR/kW) and higher BES costs, where BES achieves higher savings than in the base case. An additional particularly interesting marginal result is observed for the investment cost pair of 1400/50, where only BES is utilized, achieving an optimal capacity of 234.94 kWh while PV capacity is zero. In this scenario, BES alone is sufficient to maintain a positive *neg(objective function)* value of 1094.31 EUR/a.

The decrease in water demand also leads to reductions in optimal PV and BES capacities compared to the baseline, with PV capacities experiencing a larger relative decline due to the greater drop in PtW and PV revenues. While BES capacities also decrease, a slightly broader range of BES usage is observed for higher BES costs, suggesting that BES remains an important component in the system even with reduced water demand.

These comparisons emphasize the nuanced impact of reduced water demand on the optimal system. While the reductions in PtW and PV savings are more pronounced in absolute terms, BES still plays a stabilizing role in the system's profitability, ensuring that even under reduced water demand scenarios, the system maintains relatively close profitability to the base case.

It is further evident that the decrease in water demand that results with reductions in PV and BES capacities, and the associated savings and revenues, is less impactful compared to the changes caused by reductions in grid electricity prices or PV potential. Furthermore, the analysis confirms that a 30% decrease in water demand does not lead to any non-profitable scenarios, indicating that water demand is a less critical parameter in determining system profitability. This finding highlights the resilience of the system to variations in water demand, underscoring the stability of the optimal configurations under such changes.

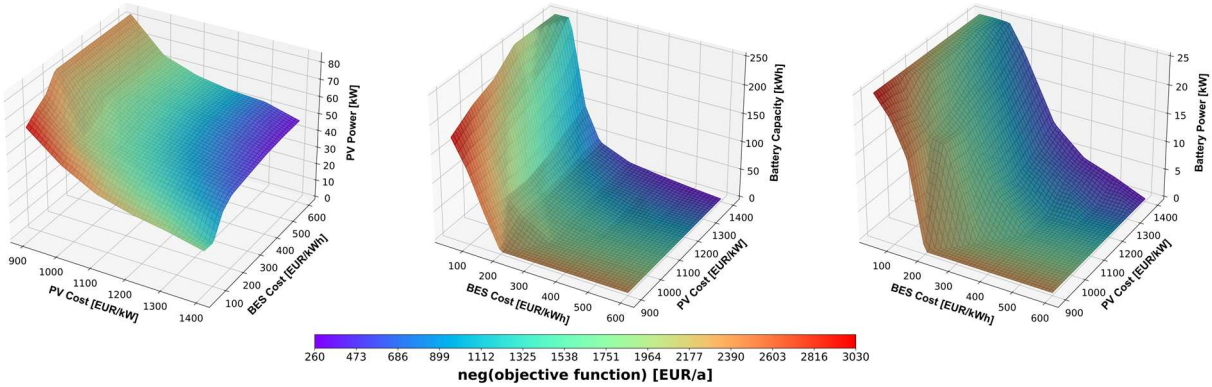


Figure 14. Range of optimal capacity results for Unije Island's water-energy system with 30% increase in water demand

When comparing the 30% increase in water demand to the base case, the *neg(objective function)* values shift from a range of [240, 2290] EUR/a in the base case to [260, 3030] EUR/a in the 30% increase scenario. This change, while notable, is smaller than the effects observed in scenarios involving grid electricity price and PV potential changes, further confirming that changes in water demand have a relatively lower effect on the total optimal system configuration and dispatch.

The higher water demand results in a more significant increase in savings and income from PtW and PV usage (in absolute terms) compared to the higher savings due to BES usage. Although there is also a noticeable increase in BES savings, the percentage increase in savings is more pronounced for PtW

and PV usage. Specifically, BES savings increase by an average of +44.6%, while PtW and PV usage savings rise by approximately +30.9%. In absolute terms, BES savings are higher by an average of 140.5 EUR/a, while PtW and PV usage savings increase by an average of 1356.27 EUR/a.

It is interesting to follow the most profitable solution in base case and compare it to the Figure 14 for an increase in water demand. The most profitable solution with *neg(objective function)* value equal to 2290 EUR/a can be closely followed by the profitable equivalent solution in water demand increase case by the orange colour. The closest *neg(objective function)* equal solutions for increase in water demand are seen at PV/BES investment cost pairs of 1000/118 with value of 2286.64 EUR/a, and at pair 1100/50 with 2283.81 EUR/a *neg(objective function)* value.

Overall, there is a noticeable increase in both PtW and BES revenues, with a higher average absolute increase for PtW and PV usage. However, the percentage increase in savings and earnings is higher for BES usage. As BES is deployed at higher PV costs and lower BES costs, with quite high capacities (on average 240 kWh), it is evident that with an increase in water demand and, consequently, electricity consumption for desalination, there is limited additional room for savings through BES for these cost pairs. This is because the savings are already relatively high, driven by the system nearing the upper BES capacity limit.

It is evident that both PV and BES capacities are higher than in the base case, indicating that the increase in water demand similarly affects the optimal PV and BES capacities. However, it is more noticeable that the impact on PV is slightly more pronounced, leading to a greater increase in optimal PV capacities. This, in turn, results in an increase in savings associated with the slightly higher PV output. The red area, representing the most unprofitable solutions across all optimal combinations, is located at the lowest PV cost, further emphasizing the significance of PV in this scenario.

Compared to the base case, although BES capacities are also higher, the range of BES usage is marginally greater for higher BES costs. This can be observed in the case of higher PV costs, where BES remains a viable option at higher BES costs, such as the cost combinations of 1300/450 or 1400/500, where BES would not have been optimal in the base case. However, it is important to note that the differences in the absolute values of BES capacity are minimal, meaning they have little impact on final profitability.

In conclusion, the primary impact on the increase in both PV and BES capacities, which leads to higher savings and income from both sources, is less significant compared to the effects of changes in other parameters. Thus, while the increase in PV and BES capacities contributes to profitability, it is the changes in other factors, such as grid electricity prices and PV potential, that have a more substantial effect on overall system performance.

5. Conclusion and future work

This study introduces the framework for optimizing integrated water-energy systems, applied to small-scale island with unique seasonal fluctuations. The research significantly advances the traditional approach by implementing a MILP model that not only determines the optimal capacities for RES and BES but also integrates these with water supply systems via a RO desalination unit and water storage highlighting the importance of PtW. Furthermore, unlike the traditional approach in water-energy system analyses, which often focuses solely on BES capacity optimization, this study adopts a more detailed methodology considering both BES capacity and power rating as variables.

This dynamic optimization framework contrasts with conventional methods that typically rely on predetermined capacities, instead offering a comprehensive strategy to optimize both system capacity and dispatch in response to varying energy and water demands on a yearly basis. The methodological approach is grounded in a MILP optimisation model, which facilitates the simultaneous optimization of multiple variables across interconnected energy and water systems. Additionally, the proposed RES

and BES range investment cost analysis enables a robust approach that can accommodate market volatility and technological advancements.

The case study of Unije Island underscores the practical applicability of the proposed model, demonstrating its effectiveness in optimizing an integrated water-energy system within a context characterized by seasonal population spikes due to tourism and a variable climate. The optimization results reveal the potential for enhanced system flexibility and economic performance, particularly through the deployment of PtW technologies and the efficient management of energy and water storage. The insights gained from this case study are not only applicable to the specific context of Unije Island but also offer broader implications for the optimization of water-energy systems on other islanded or remote areas.

The study comprehensively mapped how variations in investment cost impact system operation, financial viability, and broader economic outcomes, revealing a complex relationship between RES power generation and storage options. Significant observation was the non-linear influence of BES investment costs on the optimal PV power capacities. While lower PV costs generally incentivize higher PV power capacities, the rate of this increase is dependent on the BES investment costs. The study also highlights the importance of BES capacity and power as separate but interdependent variables in optimizing the system's performance.

The findings demonstrated that BES capacity influences not only the overall storage potential but also the required BES power, which must be adequately matched to avoid underutilization or overestimation of storage capabilities. This is particularly evident in scenarios where BES power follows the capacity trend, but with sharper changes, especially at lower PV investment costs. These results underscore the importance of treating BES power and capacity as distinct parameters in the optimization process to achieve accurate and efficient system configurations. Moreover, the analysis of BES utilization gives additional view on optimal storage usage. While high BES utilization is typically associated with efficient storage operation, the results indicated that maximum financial and economic benefits might not necessarily coincide with maximum BES usage. In fact, the highest objective function values, indicative of the most financially and economically optimal configurations, were observed at lower BES utilization levels. This counterintuitive finding, together with the findings showing decrease in optimal PV power with lower BES investment cost, suggests that the optimal integration of PV and BES does not simply depend on maximisation of PV and storage capacities but rather on achieving the right combination that maximizes financial and economic returns while minimizing costs.

Furthermore, the flexible operation savings, which capture the combined economic benefits of both PtW and BES storage, underscore the importance of integrating these technologies in a balanced manner. The highest flexible operation savings are achieved when both PV and BES investment costs are minimized, indicating that cost reductions in both areas are essential for maximizing system efficiency. Moreover, the results show that the PV savings and earnings decrease as BES capacity increases, particularly when BES investment costs are low. This trend further highlights the trade-off between direct PV utilization and storage options. Thus, the optimal system design must carefully balance these factors to achieve the greatest overall savings and earnings.

The results further highlight the sensitivity of the water-energy system's optimal configuration to changes in grid electricity price, PV potential, and water demand. Results indicate that an increase in grid electricity prices enhances the system’s profitability by incentivizing the use of PV and PtW further reducing reliance on grid electricity. Higher PV potential leads to increased PV installation, improving renewable energy utilization and overall system performance. Conversely, lower grid electricity prices or reduced PV potential diminish economic viability, shifting reliance to BES and raising operational costs. Furthermore, decrease in both grid electricity prices and PV potential in some investment cost pair combinations resulted with the non-profitable solution marking those parameter changes as critical.

Changes in water demand primarily influence the capacity requirements of system components. Higher demand necessitates scaling up both energy and water system capacities, which impacts revenues and

operational strategies. Lower demand reduces system load but may affect cost efficiency due to underutilized infrastructure. However, and contrary to grid electricity price and PV potential change, decrease in water demand does not result with non-profitable solutions which marks water demand as non-critical parameter. These findings emphasize the need for tailored strategies to adapt to varying cost and resource scenarios, ensuring optimal system performance and economic efficiency.

The contributions of this research extend beyond theoretical advancements, offering practical solutions and a versatile modelling framework that can be adapted to various areas. Furthermore, the findings provide valuable guidance for policymakers and stakeholders involved in the sustainable development of island communities, particularly in the face of evolving energy markets and climate challenges. Future research will expand this framework to include additional renewable energy sources, water production technologies, and additional external economical benefits, thereby enhancing its utility across a wider range of scenarios. Additionally, crucial input parameters change in future research will aim to show the effect on optimal solution distribution further increasing the robustness of the proposed modelling framework.

Abbreviations

Acronyms

EU	-	European Union
RES	-	Renewable energy sources
PV	-	Photovoltaic power plant
RO	-	Reverse osmosis desalination unit
BES	-	Battery energy storage
DSM	-	Demand-side management
PSO	-	Particle swarm optimisation
MILP	-	Mixed integer linear programming
PtW	-	Power-to-Water
MIQCP	-	Mixed-integer quadratically-constrained programming
SOC	-	State of charge
RHS	-	Right hand side
LHS	-	Left hand side

Nomenclature

Model sets

Name	**Description**
$t \in T$	Time periods
$pvc \in PVC$	PV power investment cost change
$bc \in BC$	Battery storage capacity investment cost change
$pc \in PC$	Important parameters
$\varepsilon \in \Omega_E$	Grid electricity price change
$\kappa \in \Omega_K$	PV potential change
$\psi \in \Omega_\Psi$	Water demand change

Model variables

Name	**Unit**	**Description**
$LL_{pvc,\,bc,\,t}$	kWh	Lost load
$G^{D}_{pvc,\,bc,\,t}$	kWh	Grid energy used for desalination electricity demand
$B^{DC}_{pvc,\,bc,\,t}$	kWh	Battery discharging
$B^{CH,G}_{pvc,\,bc,\,t}$	kWh	Battery charging from the grid
$B^{CH,PV}_{pvc,\,bc,\,t}$	kWh	Battery charging from available PV generation
$B^{SOC}_{pvc,\,bc,\,t}$	kWh	Battery state of charge

$B^{P}_{pvc, bc, t}$	kW	Battery power output
$PV^{D}_{pvc, bc, t}$	kWh	PV power used for the desalination electricity demand
$PV^{G}_{pvc, bc, t}$	kWh	PV power transferred to the grid
$PV^{E}_{pvc, bc, t}$	kWh	PV generation
$X^{PV}_{pvc, bc, t}$	{1,0}	Binary variable allowing PV battery charging
$X^{G}_{pvc, bc, t}$	{1,0}	Binary variable allowing grid battery charging
$X^{DC}_{pvc, bc, t}$	{1,0}	Binary variable allowing battery discharging
$E^{D}_{pvc, bc, t}$	kWh	Electricity demand
$B^{NP}_{pvc, bc}$	kW	Optimal battery power
$B^{C}_{pvc, bc}$	kWh	Optimal battery capacity
$PV^{P}_{pvc, bc}$	kW	Optimal PV power
$W^{L}_{pvc, bc, t}$	m^3	Water level values
$W^{D}_{pvc, bc, t}$	m^3	Water production
$W^{B}_{pvc, bc, t}$	m^3	Water boat carriers

Model parameters

Name	**Unit**	**Description**
ll^{c}	EUR/kWh	Lost load cost
e^{P}_{t}	EUR/kWh	Grid electricity price profile
e^{S}_{t}	EUR/kWh	Selling electricity price profile
pv^{S}_{t}	kWh/kW	PV power potential
pv^{C}_{pvc}	EUR/kW	PV power investment cost
pv^{var}	EUR/kWh	Variable PV cost
b^{CC}_{bc}	EUR/kWh	Battery storage capacity investment cost
b^{MCC}	EUR/kWh/a	Battery storage capacity maintenance cost
b^{PC}_{bc}	EUR/kW	Battery storage power investment cost
b^{MPC}	EUR/kW/a	Battery storage power maintenance cost
$b^{P, min}$	kW	Minimum battery power
$b^{P, max}$	kW	Maximum battery power
$b^{ch,\eta}$	%	Battery charge efficiency
$b^{dc,\eta}$	%	Battery discharge efficiency
b^{soc}_{t0}	%	Battery state of charge in the first time step in %
$b^{soc, min}$	%	Minimum battery state of charge in %
$b^{soc, max}$	%	Maximum battery state of charge in %
b^{sd}	%/month	Battery self-discharge
w^{D}_{t}	m^3	Water demand
w^{LC}	m^3	Water storage capacity
w^{L}_{t0}	%	Water level in the first time step in %
$w^{L,max}$	%	Maximum water level in %
$w^{L,min}$	%	Minimum water level in %
w^{BC}	EUR/m^3	Water boat carrier cost
d^{η}	kWh/m^3	Water production or treatment specific energy consumption
d^{c}	m^3/h	Water production or treatment unit nominal capacity
lf	years	Life-time of a technology
ry	year	Battery storage replacement year
dr	%	Discount rate
cr	-	Capital recovery factor
icdf	-	Battery storage investment cost decrease factor
pvf	-	Present value factor
Δt	h	Time-step in units of hour
γ	-	Ratio of electricity selling and purchase price

Acknowledgments

Contributions from companies Vodoopskrba i odvodnja Cres Lošinj d.o.o. and Ericsson Nikola Tesla d.d. regarding the data availability for the Unije Case study is greatly acknowledged. Furthermore, the contributions from European Union's Horizon Europe programme projects INITIATE, Grant agreement ID 101136775, as well as from the project EMERGE, Grand agreement ID 101118278 are greatly acknowledged.

Reference

[1] Directorate-General for Energy (European Commission). Clean energy for all Europeans. 2019. https://doi.org/10.2833/9937.

[2] European Commission. A Framework Strategy for a Resilient Energy Union with a Forward-Looking Climate Change Policy /* COM/2015/080 final */. n.d.

[3] Kotzebue JR, Weissenbacher M. The EU's Clean Energy strategy for islands: A policy perspective on Malta's spatial governance in energy transition. Energy Policy 2020;139:111361. https://doi.org/10.1016/j.enpol.2020.111361.

[4] Initiative SI. Smart Islands Declaration. n.d.

[5] European Commission. Clean energy for EU islands n.d. https://ec.europa.eu/energy/topics/markets-and-consumers/clean-energy-eu-islands_en.

[6] Duić N, Krajačić G, da Graça Carvalho M. RenewIslands methodology for sustainable energy and resource planning for islands. Renew Sustain Energy Rev 2008;12:1032–62. https://doi.org/10.1016/j.rser.2006.10.015.

[7] Pfeifer A, Dobravec V, Pavlinek L, Krajačić G, Duić N. Integration of renewable energy and demand response technologies in interconnected energy systems. Energy 2018;161:447–55. https://doi.org/10.1016/j.energy.2018.07.134.

[8] Dorotić H, Doračić B, Dobravec V, Pukšec T, Krajačić G, Duić N. Integration of transport and energy sectors in island communities with 100% intermittent renewable energy sources. Renew Sustain Energy Rev 2019;99:109–24. https://doi.org/10.1016/j.rser.2018.09.033.

[9] Dominković D, Stark G, Hodge B-M, Pedersen A. Integrated Energy Planning with a High Share of Variable Renewable Energy Sources for a Caribbean Island. Energies 2018;11:2193. https://doi.org/10.3390/en11092193.

[10] Groppi D, Pfeifer A, Garcia DA, Krajačić G, Duić N. A review on energy storage and demand side management solutions in smart energy islands. Renew Sustain Energy Rev 2021;135:110183. https://doi.org/10.1016/j.rser.2020.110183.

[11] Maleki A. Design and optimization of autonomous solar-wind-reverse osmosis desalination systems coupling battery and hydrogen energy storage by an improved bee algorithm. Desalination 2018;435:221–34. https://doi.org/10.1016/j.desal.2017.05.034.

[12] Triantafyllou P, Koroneos C, Kondili E, Kollas P, Zafirakis D, Ktenidis P, et al. Optimum green energy solution to address the remote islands' water-energy nexus: the case study of Nisyros island. Heliyon 2021;7:e07838. https://doi.org/10.1016/j.heliyon.2021.e07838.

[13] Moazeni F, Khazaei J, Pera Mendes JP. Maximizing energy efficiency of islanded micro water-energy nexus using co-optimization of water demand and energy consumption. Appl Energy 2020;266:114863. https://doi.org/10.1016/j.apenergy.2020.114863.

[14] Valencia-Díaz A, Toro EM, Hincapié RA. Optimal planning and management of the energy–water–carbon nexus in hybrid AC/DC microgrids for sustainable development of remote communities. Appl Energy 2025;377:124517. https://doi.org/10.1016/j.apenergy.2024.124517.

[15] Santhosh A, Farid AM, Youcef-Toumi K. The impact of storage facility capacity and ramping capabilities on the supply side economic dispatch of the energy–water nexus. Energy 2014;66:363–77. https://doi.org/10.1016/j.energy.2014.01.031.

[16] Kyriakarakos G, Dounis AI, Rozakis S, Arvanitis KG, Papadakis G. Polygeneration microgrids: A viable solution in remote areas for supplying power, potable water and hydrogen as transportation fuel. Appl Energy 2011;88:4517–26. https://doi.org/10.1016/j.apenergy.2011.05.038.

[17] Mimica M, Dominković DF, Capuder T, Krajačić G. On the value and potential of demand response in the smart island archipelago. Renew Energy 2021;176:153–68. https://doi.org/10.1016/j.renene.2021.05.043.

[18] Stoppato A, Cavazzini G, Ardizzon G, Rossetti A. A PSO (particle swarm optimization)-based model for the optimal management of a small PV(Photovoltaic)-pump hydro energy storage in a rural dry area. Energy 2014;76:168–74. https://doi.org/10.1016/j.energy.2014.06.004.

[19] Perković L, Novosel T, Pukšec T, Ćosić B, Mustafa M, Krajačić G, et al. Modeling of optimal energy flows for systems with close integration of sea water desalination and renewable energy sources: Case study for Jordan. Energy Convers Manag 2016;110:249–59. https://doi.org/10.1016/j.enconman.2015.12.029.

[20] Jannesar MR, Sedighi A, Savaghebi M, Guerrero JM. Optimal placement, sizing, and daily charge/discharge of battery energy storage in low voltage distribution network with high photovoltaic penetration. Appl Energy 2018;226:957–66. https://doi.org/10.1016/j.apenergy.2018.06.036.

[21] Sedghi M, Ahmadian A, Aliakbar-Golkar M. Optimal Storage Planning in Active Distribution Network Considering Uncertainty of Wind Power Distributed Generation. IEEE Trans Power Syst 2016;31:304–16. https://doi.org/10.1109/TPWRS.2015.2404533.

[22] Huang Y, Li P, Wang W, Dong L. Capacity Optimization of Battery Energy Storage System in Multi-energy Complementary System Based on Time Series Simulation Method. 2019 IEEE Innov. Smart Grid Technol. - Asia (ISGT Asia), IEEE; 2019, p. 3804–9. https://doi.org/10.1109/ISGT-Asia.2019.8881502.

[23] Grover-Silva E, Girard R, Kariniotakis G. Optimal sizing and placement of distribution grid connected battery systems through an SOCP optimal power flow algorithm. Appl Energy 2018;219:385–93. https://doi.org/10.1016/j.apenergy.2017.09.008.

[24] Li P, Huang Y, Qi W, Gan J. Capacity Co-Optimization of Thermal and Battery Energy Storage System in Multi-energy Complementary System. 2019 IEEE Innov. Smart Grid Technol. - Asia (ISGT Asia), IEEE; 2019, p. 3815–9. https://doi.org/10.1109/ISGT-Asia.2019.8881407.

[25] Ogunmodede O, Anderson K, Cutler D, Newman A. Optimizing design and dispatch of a renewable energy system. Appl Energy 2021;287:116527. https://doi.org/10.1016/j.apenergy.2021.116527.

[26] Mehrjerdi H, Aljabery AAM. Modeling and Optimal Planning of an Energy–Water–Carbon Nexus System for Sustainable Development of Local Communities. Adv Sustain Syst 2021;5. https://doi.org/10.1002/adsu.202100024.

[27] Mehrjerdi H, Aljabery AAM, Saboori H, Jadid S. Carbon-Constrained and Cost Optimal Hybrid Wind-Based System for Sustainable Water Desalination. IEEE Access 2021;9:84079–92. https://doi.org/10.1109/ACCESS.2021.3087540.

[28] Kariman H, Shafieian A, Khiadani M. Small scale desalination technologies: A comprehensive review. Desalination 2023;567:116985. https://doi.org/10.1016/j.desal.2023.116985.

[29] Ghazi ZM, Rizvi SWF, Shahid WM, Abdulhameed AM, Saleem H, Zaidi SJ. An overview of

water desalination systems integrated with renewable energy sources. Desalination 2022;542:116063. https://doi.org/10.1016/j.desal.2022.116063.

[30] Bundschuh J, Kaczmarczyk M, Ghaffour N, Tomaszewska B. State-of-the-art of renewable energy sources used in water desalination: Present and future prospects. Desalination 2021;508:115035. https://doi.org/10.1016/j.desal.2021.115035.

[31] Nurjanah I, Chang T-T, You S-J, Huang C-Y, Sean W-Y. Reverse osmosis integrated with renewable energy as sustainable technology: A review. Desalination 2024;581:117590. https://doi.org/10.1016/j.desal.2024.117590.

[32] Carta J, González J, Subiela V. The SDAWES project: an ambitious R&D prototype for wind-powered desalination. Desalination 2004;161:33–48. https://doi.org/10.1016/S0011-9164(04)90038-0.

[33] Subiela VJ, de la Fuente JA, Piernavieja G, Peñate B. Canary Islands Institute of Technology (ITC) experiences in desalination with renewable energies (1996–2008). Desalin Water Treat 2009;7:220–35. https://doi.org/10.5004/dwt.2009.733.

[34] Spyrou ID, Anagnostopoulos JS. Design study of a stand-alone desalination system powered by renewable energy sources and a pumped storage unit. Desalination 2010;257:137–49. https://doi.org/10.1016/j.desal.2010.02.033.

[35] Rosales-Asensio E, Rosales A-E, Colmenar-Santos A. Surrogate optimization of coupled energy sources in a desalination microgrid based on solar PV and wind energy. Desalination 2021;500:114882. https://doi.org/10.1016/j.desal.2020.114882.

[36] Mehrjerdi H. Modeling and optimization of an island water-energy nexus powered by a hybrid solar-wind renewable system. Energy 2020;197:117217. https://doi.org/10.1016/j.energy.2020.117217.

[37] Cabrera P, Carta JA, Matos C, Lund H. Lessons learned in wind-driven desalination systems in the Canary Islands: Useful knowledge for other world islands. Desalination 2024;583:117697. https://doi.org/10.1016/j.desal.2024.117697.

[38] Padrón I, Avila D, Marichal GN, Rodríguez JA. Assessment of Hybrid Renewable Energy Systems to supplied energy to Autonomous Desalination Systems in two islands of the Canary Archipelago. Renew Sustain Energy Rev 2019;101:221–30. https://doi.org/10.1016/j.rser.2018.11.009.

[39] Cabrera P, Carta JA, Lund H, Thellufsen JZ. Large-scale optimal integration of wind and solar photovoltaic power in water-energy systems on islands. Energy Convers Manag 2021;235:113982. https://doi.org/10.1016/j.enconman.2021.113982.

[40] Sanna A, Buchspies B, Ernst M, Kaltschmitt M. Decentralized brackish water reverse osmosis desalination plant based on PV and pumped storage - Technical analysis. Desalination 2021;516:115232. https://doi.org/10.1016/j.desal.2021.115232.

[41] Ajiwiguna TA, Lee G-R, Lim B-J, Cho S-H, Park C-D. Optimization of battery-less PV-RO system with seasonal water storage tank. Desalination 2021;503:114934. https://doi.org/10.1016/j.desal.2021.114934.

[42] Mentis D, Karalis G, Zervos A, Howells M, Taliotis C, Bazilian M, et al. Desalination using renewable energy sources on the arid islands of South Aegean Sea. Energy 2016;94:262–72. https://doi.org/10.1016/j.energy.2015.11.003.

[43] Liu Z, Zheng W, Yuan J, Zhang B, Lv B, Sun J. Optimal Configuration of Island Water-Energy Nexus Systems Considering Multistage Desalination. 2024 9th Asia Conf. Power Electr. Eng., IEEE; 2024, p. 278–83. https://doi.org/10.1109/ACPEE60788.2024.10532570.

View publication stats

[44] Clarke DP, Al-Abdeli YM, Kothapalli G. Multi-objective optimisation of renewable hybrid energy systems with desalination. Energy 2015;88:457–68. https://doi.org/10.1016/j.energy.2015.05.065.

[45] Smaoui M, Abdelkafi A, Krichen L. Optimal sizing of stand-alone photovoltaic/wind/hydrogen hybrid system supplying a desalination unit. Sol Energy 2015;120:263–76. https://doi.org/10.1016/j.solener.2015.07.032.

[46] Bilton AM, Kelley LC. Design of power systems for reverse osmosis desalination in remote communities. Desalin Water Treat 2015;55:2868–83. https://doi.org/10.1080/19443994.2014.940641.

[47] Ahmed FE, Hashaikeh R, Diabat A, Hilal N. Mathematical and optimization modelling in desalination: State-of-the-art and future direction. Desalination 2019;469:114092. https://doi.org/10.1016/j.desal.2019.114092.

[48] Okampo EJ, Nwulu N. Optimisation of renewable energy powered reverse osmosis desalination systems: A state-of-the-art review. Renew Sustain Energy Rev 2021;140:110712. https://doi.org/10.1016/j.rser.2021.110712.

[49] Ghenai C, Merabet A, Salameh T, Pigem EC. Grid-tied and stand-alone hybrid solar power system for desalination plant. Desalination 2018;435:172–80. https://doi.org/10.1016/j.desal.2017.10.044.

[50] Peng W, Maleki A, Rosen MA, Azarikhah P. Optimization of a hybrid system for solar-wind-based water desalination by reverse osmosis: Comparison of approaches. Desalination 2018;442:16–31. https://doi.org/10.1016/j.desal.2018.03.021.

[51] Meschede H. Increased utilisation of renewable energies through demand response in the water supply sector – A case study. Energy 2019;175:810–7. https://doi.org/10.1016/j.energy.2019.03.137.

[52] Mehrjerdi H. Modeling and integration of water desalination units in thermal unit commitment considering energy and water storage. Desalination 2020;483:114411. https://doi.org/10.1016/j.desal.2020.114411.

[53] Coelho L. Linearization of variable multiplication n.d. https://www.leandro-coelho.com/linearization-product-variables/.

[54] Wirtz M, Remmen P, Müller D. EHDO: A free and open-source webtool for designing and optimizing multi-energy systems based on MILP. Comput Appl Eng Educ 2021;29:983–93. https://doi.org/10.1002/cae.22352.

[55] Wirtz M. EHDO Tool - Github web page. Inst Energy Effic Build Indoor Clim RWTH Aachen Univ n.d. https://github.com/RWTH-EBC/EHDO/tree/master.

[56] Croatian Bureau of Statistics. Croatia 2021 Census. 2022.

[57] Croatian Meteorological and Hydrological Service. Weather data - Unije island n.d. https://meteo.hr/klima.php?section=klima_podaci&param=k1&Grad=mali_losinj.

[58] National Renewable Energy Laboratory. U.S. Solar Photovoltaic System and Energy Storage Cost Benchmarks, With Minimum Sustainable Price Analysis: Q1 2022. n.d.

[59] Wesley C, Akash K. Cost Projections for Utility Scale Battery Storage: 2023 Update. 2023.